POLITECNICO
MILANO 1863

SCUOLA DI INGEGNERIA INDUSTRIALE
E DELL'INFORMAZIONE

Parametric Design Tool for a GEO Mission Architecture

Tesi di Laurea Magistrale in
Space Engineering - Ingegneria Spaziale

Author: **Angelo Roberto Lannutti**

Student ID: 990741
Advisor: Prof. Michèle Roberta Lavagna
Co-advisors: Salvatore Andrea Bella
Academic Year: 2022-2023

Abstract

In this study, a groundbreaking tool for preliminary design, focusing on mass and power budgets, has been developed for general-purpose GEO satellites. This tool holds immense value for both commercial and research domains, providing a rapid overview of the overall budgets for various satellite types intended for operation in GEO orbit, including those outside the conventional applications like Communications, Navigation, and Meteorology.

The tool addresses a critical gap in current data availability, particularly for non communication satellites in GEO, making it an essential asset for the design and analysis of diverse satellite missions. It extracts relevant subsystem budget data from the literature, assuming that certain features and dimensions of classical GEO satellites remain consistent. The Propulsion Subsystem and the Electric Power Subsystem are explicitly modeled, requiring user input for various parameters, along with payload mass and power, which play a pivotal role in determining the satellite class.

The thesis comprises a literature review, offering insights into existing tools and studies related to GEO satellite mass and power budgets. The main body provides a concise overview of the modeled subsystems, the algorithm's functioning, and the tool's validation. The concluding section features several case studies, including hypothetical applications of the tool in designing In-Orbit Servicing missions, drawing inspiration from NASA projects.
Keywords: GEO, In-Orbit servicing, mass budget, power budget, system engineering, system design

Abstract in lingua italiana

In questo studio è stato sviluppato uno strumento innovativo per la progettazione preliminare di satelliti GEO ad uso generale, con un focus su budget di massa, potenza e costi. Questo strumento è di grande valore sia per il settore commerciale che per quello della ricerca, fornendo una panoramica rapida dei budget complessivi per vari tipi di satelliti destinati all'orbita GEO, inclusi quelli al di fuori delle applicazioni convenzionali come Comunicazioni, Navigazione e Meteorologia.

Lo strumento affronta una lacuna critica nella disponibilità attuale di dati, in particolare per i satelliti non di comunicazione in orbita GEO, rendendolo un asset essenziale per la progettazione e l'analisi di diverse missioni satellitari. Estrae dati rilevanti dal budget dei sottosistemi dalla letteratura, assumendo che alcune caratteristiche e dimensioni dei satelliti GEO classici rimangano coerenti. I sottosistemi di propulsione e di alimentazione elettrica sono esplicitamente modellati, richiedendo l'input dell'utente per vari parametri, insieme a massa e potenza del carico utile, che giocano un ruolo cruciale nella determinazione della classe del satellite.

La tesi comprende una revisione della letteratura, offrendo approfondimenti sugli strumenti esistenti e sugli studi correlati ai budget di massa e potenza dei satelliti GEO. Il corpo principale fornisce una panoramica sintetica dei sottosistemi modellati, del funzionamento dell'algoritmo e della validazione dello strumento. La sezione conclusiva presenta diversi casi studio, che includono applicazioni ipotetiche dello strumento nella progettazione di missioni di servicing in orbita, che prendono ispirazione da progetti della NASA.
Parole chiave: Orbita Geostazionaria, Dimensionamento preliminare, Budget di massa, Budget di potenza, Ingegneria dei sistemi, progettazione di missione.

Contents

Acronyms

ADCS Attitude Determination and Control Subsystem. 5, 10, 18–20, 31, 33, 62, 63, 68

AR&C Autonomous Rendez-vous and Capture. 51–58, 61, 62, 64

DARPA Defense Advanced Research Projects Agency. 54

DOF Degree of Freedom. 54

ECSS European Cooperation for Space Standardization. 34

EPS Electric Power Subsystem. 3, 10, 16, 59

ESA European Space Agency. 34

FREND Front-end Robotics Enabling Near-term Demonstration. 54

GEO Geostationary orbit. 3–5, 9, 10, 12, 17–19, 26, 28–33, 35, 37, 38, 40, 43, 46, 49, 51, 52, 55, 57–60, 62, 65–67, 69, 79

GOES Geostationary Operational Environmental Satellite. 51, 55

GTO Geosynchronous Transfer Orbit. 10, 26, 28, 29, 40, 47, 57–60, 65, 69, 79

IDL Integrated Design Laboratory Robot Arm. 54

IOS In Orbit Servicing. 3, 4, 9, 12, 18, 19, 22–24, 37, 43, 51, 59, 65, 67, 68

LIDAR Laser Imaging Detection and Ranging. 53

NASA National Astronautics and Space Administration. 4, 51–53, 55, 56, 60, 61, 63, 65, 67, 77

NIST National Institute of Standards and Technology. 27

OBDH On Board Data Handling. 18–20, 31, 33

P/L Payload. 32, 33

PPU Power Processing Unit. 27

PS Propulsion Subsystem. 3, 22, 26, 49, 59

SDM Statistical Design Model. 8, 11, 37, 38, 77

SDO Solar Dynamics Observatory. 51, 55

SMAD Space Mission Analysis and Design. 3, 10, 17, 31, 32, 37, 44, 45, 79

SMOC Servicing Mission Operations Center. 52, 55

SPENVIS SPace ENVironment Information System. 69

TCS Thermal Control Subsystem. 5, 17–19, 30

TTMTC Tracking, Telemetry and Telecommmand Subsystem. 17, 18, 30, 31, 68

TWTA Travelling Wave Tube Amplifier. 39

Introduction

The aim of this thesis is to provide Systems Engineers with a practical tool for determining preliminary mass and power budgets when designing satellites in Geostationary orbit (GEO). The New Space Economy's expansion has led to the need for satellites, including those for In Orbit Servicing (IOS), in GEO orbit. These satellites differ in dimensions and power consumption from traditional Telecommunication satellites in GEO. Currently, there is a lack of literature that enables accurate estimation of subsystems' mass and power for this new class of spacecraft. This knowledge gap hampers the development of innovative missions in the private sector, acting as a barrier to growth for private companies in the Space industry. Additionally, even when a significant number of new concept satellites are launched, data may not be available due to the competitive advantage they provide to the owning company.

Commonly used methods for preliminary parametric design of GEO satellites rely on statistical approaches, as detailed in the next section. In this work, an analytical approach is applied to the most crucial subsystems (EPS, PS) due to their sensitivity to the final architecture budgets. The statistical approach is used for subsystems that do not significantly differ from Telecommunication Satellites from a conceptual standpoint.

Typical statistical regressions from GEO satellites datasets, as found in references such as the Space Mission Analysis and Design (SMAD) book[64], are insufficiently accurate for preliminary sizing if the mission's purpose differs significantly from the known mission concepts. For instance, in a IOS refueling mission, the payload is the fuel to be delivered to the client satellite, having no power consumption. Existing statistical regressions linking payload mass and total power do not account for powerless payloads, leading to inaccurate relations.

This thesis introduces an iterative method that utilizes payload mass, power, and a combination of statistical regressions from previous works in the initial iteration. Subsequent steps refine the budget with Electric Power Subsystem (EPS) and Propulsion Subsystem (PS) sizing, employing designated inputs and assumptions derived from commonly used GEO platforms, aiming for convergence between consecutive iterations. This iterative

approach grants system engineers the freedom to adjust tool settings and assumptions, allowing customization to specific needs and easy tracing of parameter effects. Unlike multidisciplinary optimization or AI-generated solutions, this approach provides flexibility and maintains validity even with limited information about payloads. Variance analysis on inputs can be performed to identify potential errors due to reverse engineering of the payload without compromising validity.

This tool aims for higher accuracy than existing statistical relations, demanding more inputs for common mission concepts. However, its primary advantage lies in its flexibility, allowing evaluation of new concept satellites and resulting in lower average relative errors in preliminary sizing compared to conventional methods.

The thesis is structured as follows:
In the first chapter, a review of existing statistical preliminary design tools for GEO communication satellites and a brief mention of other analytical preliminary design tools. Additionally, a comparison of chosen statistical relations based on a 30-satellites dataset is provided.

The second chapter offers an overall presentation of the algorithm and introduces modeling equations for EPS and PS subsystems, along with related assumptions. Statistical data for other subsystems and associated assumptions are also discussed.

In the third chapter, the tool is tested, and results are presented, including a comparison with existing statistical relations relevant to the study's scope.

The fourth chapter explores two different case studies on possible In Orbit Servicing (IOS) missions, including a deorbiting mission and a refueling mission. A comparison with budgets obtained by a National Astronautics and Space Administration (NASA) expert team for the two cases is provided. The chapter concludes with the development of a different mission concept and a final trade-off analysis on propulsion type and launcher insertion orbit. The cases report different levels of payload masses.

Finally, the fifth chapter presents conclusions and outlines potential future developments.

1 | A review on statistical Preliminary Design

Traditionally, the preliminary design of satellites relies on existing literature and data pertaining to satellites within the same category. Attempts to create codes for estimating subsystem budgets have predominantly followed a statistical design approach. However, these methods lose their validity when applied to satellites like In-Orbit servicing ones, which serve a radically different purpose and feature payloads distinct from those in the GEO database used for the model.

In the conventional design approach for complex systems, companies organize engineering groups aligned with specific disciplines, parts, or processes contributing to the system's development. These groups typically have authority over design issues within their domains and employ their own methods and software tools. Interfaces are often determined by experts and provided manually, especially in companies lacking concurrent design facilities. Consequently, true concurrency in the design process is not fully achieved, as the design of different elements proceeds sequentially. Even when concurrent design facilities are available, interactions between factors (i.e., design variables), customer requirements, and optimization goals are challenging to detect if factors are tested using an unstructured trial-and-error approach, one factor at a time[48].

Some works have proposed mathematical models to analyze complex subsystems and examine their mutual interactions. For instance, in one such work, authors introduced a structured parametric approach employing fractional factorial design, response surfaces, and statistical analysis of variance to provide the design team with graphical information on factor main effects, interactions, sensitivity to factor variations, and robustness of different architectures during early development stages[48]. However, for the purposes of this thesis, a detailed mathematical model of interactions among all subsystems may be redundant due to common features shared by subsystems like Attitude Determination and Control Subsystem (ADCS) and Thermal Control Subsystem (TCS) in satellites of the same class, once the orbit (in this case, GEO orbit) is selected.

In this context, a more in-depth analysis was conducted on publications enabling a statistical preliminary design of GEO satellite budgets. The aim was to extract statistical relations essential for determining the algorithm's exit condition and for subsystems not analytically modeled. Notable works in this area include "FADSat: A system engineering tool for the conceptual design of geostationary Earth orbit satellites platform" and "System Analysis and Design of the Geostationary Earth Orbit All-Electric Communication Satellites"[34, 41]. These publications provided valuable insights into statistical relations crucial for the algorithm's functioning and handling non-analytically modeled subsystems.

1.1. FADSat: a first try of statistical model for preliminary design

Regarding the increasing utilization of satellite platforms in geostationary orbit, a system engineering tool named FADSat[34] has been developed to streamline the conceptual design phase, thereby reducing the prohibitive costs and time associated with it. FADSat is capable of designing geostationary Earth orbit satellite platforms within the mass range of 1000–7000 kg. The key feature of FADSat lies in its ability to determine the conceptual design of the satellite platform with high efficiency and acceptable accuracy.

FADSat facilitates the extraction of structural characteristics, attitude determination and control parameters, command and data handling specifications, electrical power requirements, and other subsystem details of a satellite. Initially, the tool employs a statistical design model to provide a rough estimation of the satellite design, swiftly extracting budgets for subsystem mass, power, dimensions, and satellite cost. Subsequently, it utilizes a parametric design model approach for a more precise subsystem design, establishing component specifications from a catalog of products and corresponding manufacturers.

In this tool, the design for a GEO mission architecture starts with a statistical design approach to obtain initial budgets. Subsequently, a parametric approach is applied specifically to the EPS and PS subsystems. Unlike the FADSat model, where the statistical model was used for the first draft of every subsystem, this approach combines statistical estimation of mass and power for various subsystems with parametric design for EPS and PS subsystems.

The linear regressions employed in this work are based on a database comprising 462 geostationary Earth orbit communication satellites (representing 30 different geostationary Earth orbit satellite platforms) launched between 2000 and 2017, ranging from 1000 to 7000 kg in total mass[34]. The statistical design model developed in this framework

is also used as a reference for validating the tool, with some of its relations integrated into the algorithm. This integration enhances the precision of the output and flexibility in modeling various satellite types beyond communication satellites. The statistical relations developed are presented in Figures 1.1 and 1.2.

Model	Relation
NoT – BW	$NoT = 0.0276 \times BW$
NoT – NCR	$NoT = 0.166 \times NCR$
NoT – DR	$NoT = 0.011 \times DR$
$M_T - NoT$	$M_T = 84 \times NoT - 238$
NoT 36 MHz – M_T	$NoT = 0.012 \times M_T + 2.86$
NoT 72 MHz – M_T	$NoT = 0.009 \times M_T - 1.5$
$M_T - M_{Pay}$	$M_T = 11.9 \times M_{pay} - 415$
$M_D - M_T$	$M_D = 0.553 \times M_T + 20$
$M_D - M_T$ (Feedback)	$M_D = 0.483 \times M_T + 19$
$P_T - M_D$	$P_T = 4.15 \times M_D - 1665$
$P_T - M_D$(Feedback)	$P_T = 0.966 \times M_D + 33$
$V_T - M_T$	$V_T = 4.6 \times e^{0.0005 M_T}$
$V_T - M_T$ (Feedback)	$V_T = 0.013 \times M_T - 19$
$C_{sat} - M_T$	$C_{sat} = 25.4 \times e^{0.0005 M_T}$
$C_{sat} - M_T$ (Feedback)	$C_{sat} = 0.98 \times M_T + 234$
$C_{GS} - C_{sat}$	$C_{GS} = 1.5714 \times C_{sat}$
$C_L - C_{sat}$	$C_L = 0.7857 \times C_{sat}$
$C_A - C_{sat}$	$C_A = 0.2142 \times C_{sat}$

Notation

BW	band width (MHz)
C_A	assurance cost (M$)
C_{GS}	ground segment cost (M$)
C_L	lunch cost (M$)
C_{sat}	satellite cost (M$)
DR	data rate (Mbps)
M_{ADCS}	ADCS mass (kg)
M_{CDH}	C&DH subsystem mass (kg)
M_{Com}	communication subsystem mass (kg)
M_D	dry mass (kg)
M_p	payload mass (kg)
M_{PGS}	power subsystem mass (kg)
M_{Pro}	propulsion subsystem mass (kg)
M_{STR}	structure subsystem mass (kg)
M_T	total mass (kg)
M_{TCS}	thermal subsystem power (W)
NCR	number of channel requirement
NoT	number of transponder
P_{ADCS}	ADCS power (W)
P_{CDH}	C&DH subsystem power (W)
P_{Com}	communication subsystem power (W)
P_{PGS}	power subsystem power (W)
P_{Pro}	propulsion subsystem power (W)
P_T	total power (W)
P_{TCS}	thermal subsystem mass (kg)
V_T	total volume of satellite (m^3)

Figure 1.1: System level statistical relations (left) and the relative notation (right). [34]

Subsystem	Parameter	Relation
ADCS	Mass	$M_{ADCS} = 0.053 \times M_D + 9.34$
	Mass (Auxiliary)	$M_{ADCS} = 0.052 \times M_D + 241$
	Power	$P_{ADCS} = 0.126 \times P_t - 11.3$
	Power (Auxiliary)	$P_{ADCS} = 0.127 \times P_t + 104$
EPS	Mass	$M_{PGS} = 0.197 \times M_D - 24$
	Mass (Auxiliary)	$M_{PGS} = 0.13 \times M_D + 79$
	Power	$P_{PGS} = 0.058 \times P_t - 12$
	Power (Auxiliary)	$P_{PGS} = 0.28 \times P_t - 34.57$
TT&C	Mass	$M_{Com} = 0.061 \times M_D - 10.3$
	Mass (Auxiliary)	$M_{Com} = 0.2764 \times M_D + 156$
	Power	$P_{Com} = 0.163 \times P_t - 7.12$
	Power (Auxiliary)	$P_{Com} = 0.3147 \times P_t + 102$
STR	Mass	$M_{STR} = 0.2441 \times M_D + 17$
	Mass (Auxiliary)	$M_{STR} = 0.4127 \times M_D - 481$
	Power	$P_{STR} = 0$
C&DH	Mass	$M_{CDH} = 0.0307 \times M_D + 3.5$
	Mass (Auxiliary)	$M_{CDH} = 0.0371 \times M_D - 145$
	Power	$P_{CDH} = 0.071 \times P_t - 12$
	Power (Auxiliary)	$P_{CDH} = 0.0621 \times P_t - 211.5$
PRP	Mass	$M_{Pro} = 0.1401 \times M_D - 68.5$
	Mass (Auxiliary)	$M_{Pro} = 0.0423 \times M_D + 49$
	Power	$P_{Pro} = 0.1742 \times P_t + 24$
TCS	Mass	$M_{TCS} = 0.0631 \times M_D - 3$
	Mass (Auxiliary)	$M_{TCS} = 0.0371 \times M_D - 247$
	Power	$P_{TCS} = 0.1514 \times P_t - 9.841$
	Power (Auxiliary)	$P_{TCS} = 0.124 \times P_t + 1000$
CPS	Mass	$M_{Pay} = 0.211 \times M_D + 35.13$
	Mass (Auxiliary)	$M_{Pay} = 0.1264 \times M_D + 124.7$
	Power	$P_{Pay} = 0.26 \times P_t - 13.5$
	Power (Auxiliary)	$P_{Pay} = 0.18 \times P_t + 88$

[a]The parameters presented here are defined in the Notation.
ADCS: attitude determination and control subsystem; STR: structure subsystem; TCS: thermal control subsystem; CPS: communication payload subsystem; PRP: propulsion subsystem; EPS: electrical power subsystem; C&DH: command and data handling subsystem; TT&C: telemetry, tracking and command subsystems.

Figure 1.2: Subsystem level statistical relations. [34]

The Figures 1.1 and 1.2 also reveal that deviations from the trend within the population are modeled as feedback relations if the trend remains consistent. Specifically, system relations linking payload mass to total mass and power, as well as relations between the number of transponders and payload mass, are utilized to extract information that is challenging to obtain directly from literature. However, the thesis does not analyze the cost and volume of the satellite.

The correlation coefficients, as shown in Figure 1.3, validate the presented relations and justify their usage in this work.

In the current paper, the Statistical Design Model (SDM) serves as the initial phase of

the design process. The obtained results are then optimized in the parametric design model, constituting the second part of the algorithm. Through a Graphic User Interface, the engineer refines the design by adjusting parameters selected as degrees of freedom for each subsystem model. Finally, the engineer selects hardware components from the dataset of the tool. This approach allows for a swift and detailed Phase A design of a Geosynchronous orbit communication satellite, with relative errors evaluated through case studies not exceeding 20%[34]. However, this level of detail is beyond the scope of this work, which primarily focuses on conducting rapid and robust design assessments to investigate the main effects of high-level trade-off studies. These trade-offs are intended for mission analysis, mission operations, and propulsion system type considerations for a generic IOS Mission, once the payload specifications are known.

Model	R-squared	Correlation coefficient	Correlation type
System	0.95	0.91	Very strong
ADCS	0.85	0.83	Very strong
PRP	0.81	0.79	Very strong
STR	0.92	0.89	Very strong
EPS	0.84	0.80	Very strong
C&DH	0.86	0.85	Very strong
TT&C	0.91	0.83	Very strong
TCS	0.95	0.90	Very strong
CPS	0.86	0.85	Very strong

ADCS: attitude determination and control subsystem; STR: structure subsystem; TCS: thermal control subsystem; CPS: communication payload subsystem; PRP: propulsion subsystem; EPS: electrical power subsystem; C&DH: command and data handling subsystem; TT&C: telemetry, tracking and command subsystems.

Figure 1.3: Correlation coefficients of FADSAT Statistical Design Method.[34]

1.2. System Analysis and Design of the Geostationary Earth Orbit All-Electric Communication Satellites

In this paper, a dataset comprising 70 Geostationary communication satellites launched between 2015 and 2018 has been analyzed [2]. Statistical relations to estimate mass, power, and cost of all-electric GEO satellites were derived from this dataset. While the dataset included chemical and hybrid satellites, the relations found were specifically

applicable to all-electric satellites.

The author employed a statistical design method to extract overall satellite characteristics. In a subsequent phase, an optimal Electric Propulsion subsystem, along with ADCS and Electric Power Subsystem (EPS) subsystems, was sized for the satellites using established techniques in Space Mission Analysis and Design. The system analysis was validated using SMAD[64] book percentages of various subsystems' masses and powers, demonstrating a maximum error of 30% compared to real cases. Several test case satellites present in the dataset were considered in the analysis.

Following the dataset presentation, the paper evaluated the ΔV budget for orbit raising from Geosynchronous Transfer Orbit (GTO) to GEO, station-keeping, and attitude control maneuvers. The results suggested the XIPS electric propulsion system produced by Boeing, utilizing Xenon, as the optimal choice among the options considered.

The approach presented in this paper bears similarities to the GEOdesign Tool developed in this thesis, differing in the higher number of required inputs and the non-automatic design of the entire satellite. It provides insights into the typical trade-offs that can be made using the developed tool in a fast and reliable manner. The statistical relations retrieved and employed in this paper are utilized in the GeoDesign tool for system-level analysis and computing payload characteristics for all-electric satellites. Their usage is substantiated by the high correlation coefficient values, as depicted in Figure 1.4, in conjunction with the relations' effectiveness in the analysis.

Formula	Formula Variance	Input & Output
$Y = 65.651 \times e^{0.0409\ x}$	0.9325	Input (X): Number of transponders Output (Y): Payload mass (kg)
$Y = 1411 \times e^{0.0008\ x}$	0.9806	Input (X): Payload mass (kg) Output (Y): Satellite total mass (kg)
$Y = 3.6147 \times e^{0.0007\ X}$	0.927	Input (X): Payload mass (kg) Output (Y): Electrical power consumption of payload (kw)
$Y = 0.0034\,x + 0.9759$	0.9887	Input (X): Satellite total mass (kg) Output (Y): Electrical power consumption of satellite (kw)
$Y = 5.069\, e^{0.0006\,x}$	0.7466	Input (X): Satellite total mass (kg) Output (Y): Satellite volume (m^3)
$Y = 0.012\,x + 56.833$	0.9882	Input (X): Satellite total mass (kg) Output (Y): Satellite cost (M$)
$Y = 11.921e^{0.0005\,x}$	0.9371	Input (X): Satellite total mass (kg) Output (Y): Launcher cost (M$)

Figure 1.4: Statistical relations and correlation coefficients for all-electric GEO communication satellites.[2]

1.3. Dataset summary and models comparison

To compare the statistical relations on total mass and power found in the two articles, a dataset comprising 30 satellites was created. This dataset consisted of 10 satellites from the first statistical model (the names were not provided in the paper, but the maximum errors obtained by the model were reported, enabling identification by applying the statistical relations to satellites launched in the same period and verifying that the errors were below the specified thresholds). Additionally, 10 satellites were selected from the second statistical model, and another 10 satellites were chosen that did not belong to either of the two models. These latter satellites were outside the datasets of the papers, due to the launch date.

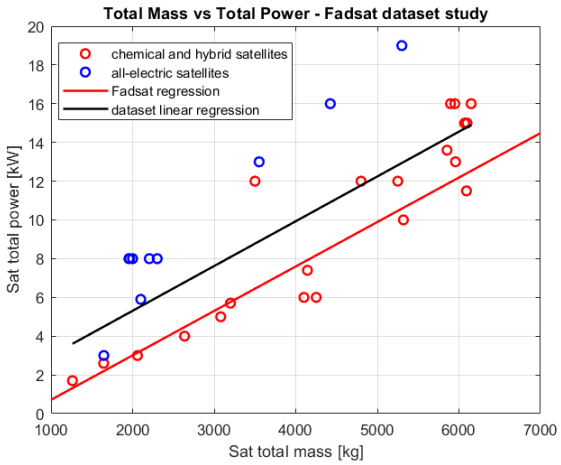

Figure 1.5: FADSAT SDM regression comparison with chemical and hybrid satellites.

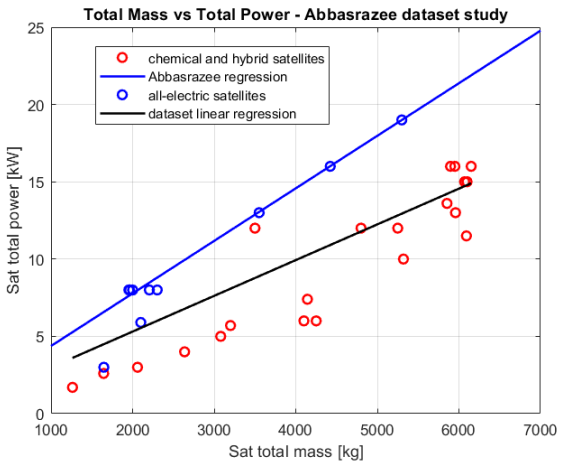

Figure 1.6: [41] statistical regression comparison with all-electric satellites.

The analysis of the datasets revealed that the first statistical model is better suited for chemical and hybrid propulsion satellites, whereas the second model is most suitable for all-electric satellites. This distinction becomes evident in Figure 1.5, where the red dots and line represent chemical and hybrid propulsion satellites with the first model's statistical regression. In contrast, the blue dots and line in Figure 1.6 depict all-electric satellites with the second model's statistical regression. The entire dataset is presented in Table 1.1. It is noticeable from the graphs that the linear regression of the entire satellite database aligns more closely with the FADSAT linear regression due to the majority of the population comprising chemical and hybrid propulsion satellites. This observation underscores the necessity of separating the applications of the two statistical models.

Consequently, in the developed tool, the statistical relations connecting payload to satellite budgets from the first model are utilized for the initial determination of total mass, total power, and dry mass when the user selects chemical or hybrid propulsion. On the other hand, the relations from the second paper are applied when electric propulsion is chosen. The statistical relations linking dry mass and total power to the mass and power of subsystems not modeled analytically in the first paper are used for both cases, assuming that these relations do not vary significantly between the two scenarios.

It's important to note that neither of these two system design techniques possesses the required flexibility to design and appropriately size a spacecraft for GEO orbit for non-communication purposes. Furthermore, the literature on IOS missions is insufficient to obtain useful statistical relations for preliminary sizing. Other tools were investigated in the present work[12, 19, 24, 26, 27, 32, 56, 66, 67], not intended for GEO IOS mission sizing, but they were not worth to be explored deeper for the scope of the work. Consequently, the demand for the newly created tool is substantial, given the increasing need for IOS satellites in the coming decades.

Table 1.1: Dataset used in the comparison. [2, 16, 25, 60, 63]

Satellite name	**Launch year**	$M_{tot}(kg)$	$P_{tot}(kW)$
ABBASRAZEE DATASET			
EUTELSAT 115 WEST B	2015	2205	8
ABS 3A	2015	1954	8
Ekspress AM8	2015	2100	5.9
ABS 2A	2016	2000	8
EUTELSAT 117 B	2016	1963	8
SES 15	2017	2302	8
Eutelsat 172 B	2017	3551	13
Angosat 1	2017	1647	3
SES 14	2018	4423	16
SES 12	2018	5300	19
SIMIL FADSAT			
Bsat 3b	2010	2060	3
Vinasat - 1	2008	2637	4
Nilesat 201	2010	3200	5.7
Athena Fidus	2014	3080	5
Palapa D	2009	4100	6
Astra 1M	2008	5320	10
MbSat1	2004	4143	7.4
Eutelsat 70B	2012	5250	12
Nstar c	2002	1645	2.6
Inmarsat 4 F2	2005	5958	13
OUT OF BOTH DATASETS			
Türksat 5A	2021	3500	12
Yahsat 1B	2021	6100	15
GSAT-11	2018	5854	13.6
Hispasat 30W-6	2018	6092	11.5
Inmarsat 5 F1	2013	6070	15
Anik F2	2004	5950	16
Measat 3b	2014	5897	16
Amos 3	2008	1263	1.7
Amos 4	2013	4250	6
Arabsat 5A	2010	4800	12

2 | Satellite model

To ensure a rapid and dependable design process, where it is feasible to monitor all potential sources of uncertainties and make adjustments to key assumptions easily, an iterative approach has been employed for the algorithm, as illustrated in Figure 2.1.

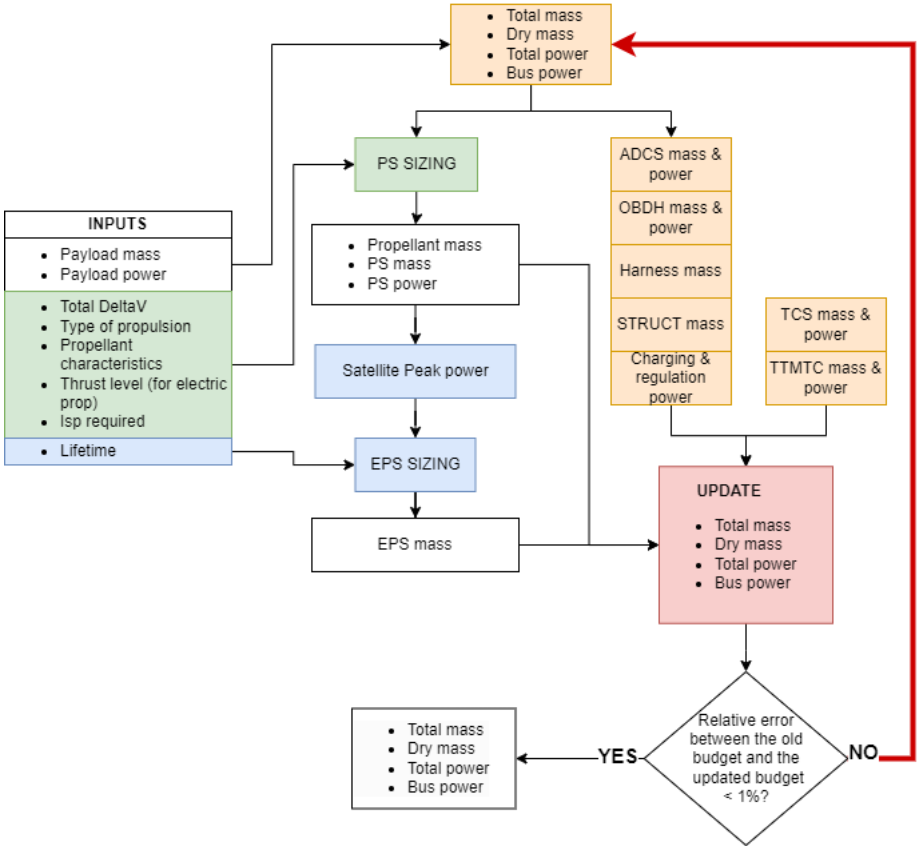

Figure 2.1: Algorithm workflow

The algorithm takes inputs as illustrated in Figure 2.1:

- Payload mass and power: These inputs are utilized to obtain an initial estimation of satellite mass and power budgets. Statistical relations presented in sections 1.1 and 1.2 are applied for hybrid or chemical propulsion satellites and all-electric satellites, respectively.

- Total ΔV, propulsion type, propellant characteristics, number of thrusters, thrust level (for electric propulsion only), and specific impulse: These inputs are employed for sizing the Propulsion subsystem.
- Expected lifetime of the satellite: This is the sole external input for the EPS subsystem, as state-of-the-art technologies have been pre-selected for its sizing, as detailed in subsequent chapters.

Once the initial parameters are estimated, the calculated dry mass is used as input for the Propulsion Subsystem sizing along with other external parameters. Assuming that the payload and the propulsion modules are not used simultaneously, the peak power is determined by comparing payload power with the propulsion subsystem power. The peak power, along with the satellite's expected lifetime, serves as input for the EPS sizing.

Additionally, the dry mass of the satellite and the bus power are used to evaluate the power and mass of the remaining subsystems, utilizing statistical relations from literature. The sum of power and mass for all subsystems provides updated total budget values. Between these budgets, a distinction has been made. The total power of the satellites comprises the payload power, the bus power of the satellites does not comprise the payload and the electric thrusters power, and the peak power of the satellite can be equal to the total power or higher, in case electric propulsion is utilized (the difference between total and peak power is due to one of the assumptions listed in the section 2.1). The new values of the peak power and of the dry mass are then compared with the previous ones. If the relative error between the old and new values exceeds 1%, the updated values become the new inputs for sizing, and the cycle repeats. This iterative process ensures accurate and reliable design while allowing flexibility for adjustments based on changing assumptions. The spacecraft subsystem models follow the scheme in the Figure 2.2.

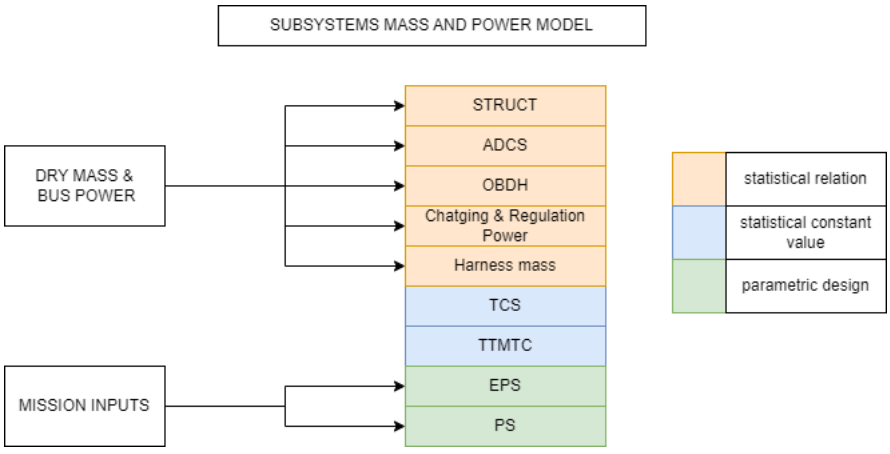

Figure 2.2: Subsystems high level modeling.

The complete workflow of the model is illustrated in Figure 2.1. The initial estimation of the total budget will be elucidated in a dedicated section, 2.2. To enhance clarity, a detailed explanation of the subsystems budgeting is imperative. The subsystems will be categorized into those modeled using statistical sizing and those modeled employing analytical sizing, as delineated by distinct colors in Figure 2.2.

2.1. Main assumptions

The main assumptions of the model can be summarized as follows:

- **SMAD reference sizings:** SMAD book reference sizings[64] are considered accurate estimates for this design phase.
- **Different relations for propulsion systems:** All-electric satellites and chemical/hybrid propulsion satellites exhibit different relationships between payload and total parameters. This aspect has been already analyzed in chapter 1.
- **GEO orbit period:** The period of the GEO orbit is assumed to be exactly 24 hours.
- **Eclipse duration:** There are 2 periods of the year in which the GEO spacecrafts are in shadows, and in these periods the eclipse lasts 72 minutes per day [37]. So, the duration of the eclipse is fixed at 4320 seconds.
- **Total power estimation:** Communication Payload power is initially estimated to be 75% of the total power based on literature database [62]. As a consequence, the bus power (here bus power is intended as the spacecrafts' subsystems power without the payload) is estimated to be 25% of the total power obtained by the GEO statistical relations, as a first estimate. The correction is possible, because the statistical relations link the total power to the dry mass and not the payload power. The substitution of the real payload power in the overall budget enables to retrieve the correct power also for the servicing satellites. The main assumption linked to this one is the subsystem features consistency.
- **Separation of subsystems:** TTMTC subsystem is considered separate from the payload in communication satellites. TTMTC and TCS units have consistent mass and power across different mission profiles, primarily dependent on the chosen orbit.
- **Payload utilization:** Being the input payload a robotic arm, a refueling system, or a communication payload, it is not utilized during the transfer phases, resulting in the peak power of the satellite being in the nominal mode for chemical satellites

or in the transfer mode for all-electric satellites.

- **Technological advancements:** Weight and power evolution of hardware due to technological advancements are not considered. The input statistical relations take partially into account the technological advancements made from 2000 to 2018 for chemical satellites [34] and from 2015 to 2018 for electric satellites [41]. However, the addition of proportional relations to make previsions for the increase or decrease in the subsystem budgets, based on the production year of the satellites, represent a further source of error for the scope of the tool, which is only intended for a preliminary sizing. These relations can then be added by the user directly on the outputs, based on the specific needs.

- **3-axis Stabilization:** Satellites are assumed to be 3-axis stabilized, a hypothesis supported by the prevalence of 3-axis stabilization in GEO satellite platforms [33, 38, 39, 58, 59]. This assumption aligns with GEO IOS mission architectures, where the servicing phase requires a 3-axis stabilized satellite[22]. Itis further strengthened by the peculiar mission needs, during the proximity operations, in which 3-axis stabilization is a strict requirement.

- **Subsystem Features Consistency:** The features of the ADCS, TTMTC, TCS, OBDH, and structural subsystems remain relatively consistent across satellites with different propulsion systems and between communication satellites used for statistical analysis and IOS satellites equipped with robotic arms. The 3-axis stabilization hypothesis for all satellites leads to similar ADCS architectures in terms of mass and power with the use of star trackers and gyroscopes for attitude determination and reaction wheels and thrusters for attitude control [33, 38, 39, 58, 59], irrespective of the mission objectives that could lead to different pointing budgets. Despite some minor changes, due to the requirements on the wheel desaturation that may be needed in case of orbit raising done with electric thrusters, the influence in the mass and power budget does not affect the design heavily. In addition, differences in the overall budgets between the chemical and electric case are already taken into account for the first iterate of the tool, so this aspect is already taken into account in the statistical data taken as reference.

  For the TTMTC subsystem (which is considered separated from the communication payload, in communication satellites), independence from mission type is assumed once the orbit is selected (only GEO orbits are considered). While data rates may vary between IOS and communication missions due to real-time telecommand requirements for proximity operations, these differences do not heavily impact the

overall subsystem architecture in terms of budgeting, given the consistent environment (GEO orbit). Communication satellites use C-band and Ku-band frequencies for Telecommand and telemetry which ensures a similar level of power, with the use of omnidirectional antennas for safe mode and directional parabolic antennas for nominal modes [33, 38, 39, 58, 59]. Similar architectures are used for IOS satellites already built [3, 22]. The addiction of a steering antenna to the servicer vehicle [22] for improved communication during proximity operations, could however induce little changes in the mass and power budgets, which are acceptable for the scope of the tool.

Similarly, the OBDH subsystem, requiring autonomous operations in IOS missions, may use more sophisticated software packages and experience higher data rates. However, the resulting differences in mass and power have a limited impact on overall budgets due to the subsystem's small scale, like shown in the biggest spacecraft management units which are in the order of 20 kg and 60 W [49].

The TCS subsystem depends solely on heat loads and orbital configuration in the absence of a three-dimensional satellite configuration, in this case the GEO orbit with no changes in the inclination. Additionally, the most thermally sensitive elements, the batteries, do not significantly differ between satellites, ensuring similar boundary conditions.

The structural subsystem design lacks peculiarities and is independent of satellite type once payload mass and subsystem masses are defined. Consistent design across diverse satellite configurations is maintained, with distinctions primarily emerging in the conceptual operations of the satellite.

- **Proportional relations:**
  - Structure subsystem mass is considered proportional to the dry mass of the satellite.
  - ADCS mass and power are proportional to total mass and power due to the need for larger reaction wheels as satellite dimensions increase. The right proportional relation, would have had the inertial properties of the spacecraft as inputs, however, this is impossible without a strong hypothesis on the configuration of the satellite, which is not the scope of the tool at this stage. However, the ADCS mass is based upon the mass and not on the inertial properties, to avoid introducing a further source of error by supposing a certain shape and mass distribution of the satellite. As the mass grows, contextually also the vol-

ume of the spacecraft grows modifying partially the inertial properties. While, the solar panels growth, is also partially taken into account by the mass growth, because it is linked to the installation of more antennas and more transponders, resulting in more power. Therefore, it is conservative to suppose that the modification of the inertial properties due to volume growth and due to the solar arrays dimension growth, is partially taken into account by a direct relation with the dry mass. An acceptable error is introduced due to the large amount of satellites present in the dataset (462 [34]) from which the relations are taken. This could lead to an overestimation of the ADCS subsystem for non-communication satellites, due to the bus power hypothesis for which the actual solar panels area can be lower than the solar panels area to which the subsystem is linked by the statistical relation, if the payload power is much lower than communication satellites typical power or it is zero. However, this effect is mitigated by the iterative process and by the uncertainty related to the relation itself.

- OBDH subsystem is proportional to dry mass and total power, reflecting the increase in spacecraft dimensions, payload capability and in the housekeeping data needed, that therefore are linked to an increase in the OBDH hardware dimensions and power.
- Harness mass is proportional to the dry mass of the spacecraft, as referenced in [17].
- Charging and Regulation power, separated from the EPS budget, is proportional to total power and its mass is included in the harness mass. The charging and regulation devices are mainly electronic components (chips, electrical interfaces), so it is right to include them in the harness mass of the spacecraft, due to the dimension and density to those elements associated.

2.2. System first estimate

As previously said, for the first estimate of the total budget of the system, different relations are implemented depending on the type of propulsion system chosen by the user. Given the payload mass and power in input, for a chemical or hybrid propulsion satellite, the following set of relations, already reported in Figure 1.1, are employed.

$$M_{tot} = M_{pay} \cdot 11.9 - 415 \tag{2.1}$$

Where M_{tot} is the total mass of the satellite and M_{pay} is the payload mass.

$$M_{dry} = M_{tot} \cdot 0.553 + 20 \tag{2.2}$$

Where M_{dry} is the dry mass of the satellite.
Differently from [34], in the model here developed, also the payload power must be given in input, so a correction is mandatory. For the total power estimate is introduced the hypothesis that the payload power accounts on average for the 75% of the total power, therefore an intermediate step of the calculation of the bus power is presented.

$$P_{bus} = (M_{dry} \cdot 4.15 - 1665) \cdot 0.25 \tag{2.3}$$

Where P_{bus} is the power of the satellite bus and the presence of the 0.25 factor has been already explained. Finally, the total power of the satellite is derived.

$$P_{tot} = P_{bus} + P_{pay} \tag{2.4}$$

Where P_{tot} is the total power of the satellite and P_{pay} is the payload power. As previously noted, P_{tot} (which more correctly represents the power required by the satellite during the payload activity mode) can be equal, in case of chemical propulsion, but also lower, in case of electric propulsion, with respect to the peak power, P_{peak} that will be used to size the solar arrays. All the mass quantities are expressed in kg and all the power quantities are expressed in W.
If the user choices the option of an all-electric satellite, the relations expressed in Figure 1.4 are implemented, following the same workflow of the previous ones and with the same correction on the bus power applied.

$$M_{tot} = 1411 \cdot exp(0.0008 \cdot M_{pay}) \tag{2.5}$$

Due to the absence of a relation that directly links the dry mass to the total mass in the set of equations shown in Figure1.4, but given the fact that this is only a first estimate and subsequent iterations will refine this value, the equation 2.2 is used also for the all-electric satellite dry mass estimation.

$$P_{bus} = (0.0034 \cdot M_{tot} + 0.9759) \cdot 0.25 \cdot 1000 \tag{2.6}$$

Where the factor 1000 derives from the fact that in the original set of equation the total power is expressed in kW. From this value, the equation 2.4 is used to retrieve the power of the nominal mode. Differently from the chemical satellites, here the power required by the electric thrusters during the transfer mode is usually higher than the payload power. As a consequence, the peak power will be retrieved with the addition of the PS power to P_{bus}.

2.3. Model limitations

Even if the use of these relations can seem wrong, due to the different purpose of the satellites in the dataset, however, **the payload mass input lies between 130 and 650 kg for the chemical and hybrid satellites and between 140 and 1500 kg for the all-electric satellites**[2, 34]. The power budgeting of the subsystems may vary

	Chemical and hybrid satellites	**All-electric satellites**
INPUT		
Payload mass	130-650 kg	140-1500 kg
Lifetime	5-18 years	5-18 years
OUTPUT		
Total mass	1000-7000 kg	1600 - 5300 kg
Total power	410 - 19000 W	7000 - 19000 W

Table 2.1: First iteration input and output nominal limitations ([2], [34])

concerning an IOS satellite, but the fundamental assumption is that the final design of the satellite bus will align with existing satellite platforms.

In the study by [34], upper and lower boundaries in dry mass and total mass for the Statistical Design Model are provided, which will be incorporated into the present tool. However, in [41], these limitations are not explicitly outlined; instead, the entire dataset is presented in a related paper[2], excluding the payload power budget. It's important to note that the tool relies on subsequent iterations that adjust the total budgets. Therefore, the constraints listed in Table 2.1 are nominal and not rigid. Acceptable results can still be achieved even within values around the boundaries.

The challenge arises in the power budget of the system, which is determined statistically. Due to the distinct characteristics of communication satellites, a different power budget might be associated with the same dry mass for IOS satellites, although no data supports this hypothesis. The scenario for all-electric satellites is distinct, as peak power is primarily determined by the power consumption of electric thrusters.

Table 2.1 does not impose any restrictions on the payload power of the satellites, as there is no explicit relation linking payload power to the total budgets of the satellites. To address the discrepancy in the ratios of payload power to the total power budget between IOS satellites (characterized by a lower ratio) and communication satellites (characterized by a higher ratio), a bus power is extracted from the total power given by the statistical relations. This extraction is performed using equations 2.6 and 2.3, and the bus power would be mostly consistent between the two satellite types, thereby avoiding potential disparities. Evidence has been found in literature[1, 3, 29, 35, 45, 65], to sustain that the payload mass range is enough for the mass of the robotic arms commonly used. For sure, the limitations on the payload mass reflect also the type of mission that can be performed, because only robotic arms of medium or large size can be used due to the lower bound imposed. Missions deploying a single tether for debris removal cannot be sized due to the too low mass, and special vehicles like depots for fuel, which do not performs any maneuvers and are peculiar in the subsystem sizing cannot be designed due to the main assumptions.

2.4. Subsystems sizing

2.4.1. PS

The sizing of the propulsion subsystem in this study constitutes the foundation of the entire parametric design, given the multitude of design parameters associated with it. This subsystem exerts the most significant influence on the total mass and power budget of spacecrafts once the mission analysis is defined. Therefore, an appropriate sizing of this subsystem forms the crux of the potential tradeoffs that a system engineer can explore.

For the sake of clarity, before delving into the specifics, a comprehensive overview of the potential alternatives for the propulsion subsystem is provided, along with the primary inputs (refer to Figure 2.3).

As depicted in Figure 2.3, four distinct designs are presented as alternatives at a low level. In reality, they can be consolidated into three, as for electric propulsion sizing, only the reference data for thruster efficiency and Propulsion Power Unit mass differ between gridded ion and Hall effect thrusters. In the case of monopropellant and bipropellant sizing, various pressure regulation techniques are hypothesized. A fully regulated pressure system is considered for the bipropellant case, while a blowdown system is assumed for the monopropellant case. These choices result in different equations and reference data.

The diverse low-level architectures proposed for propulsion are then linked to the input

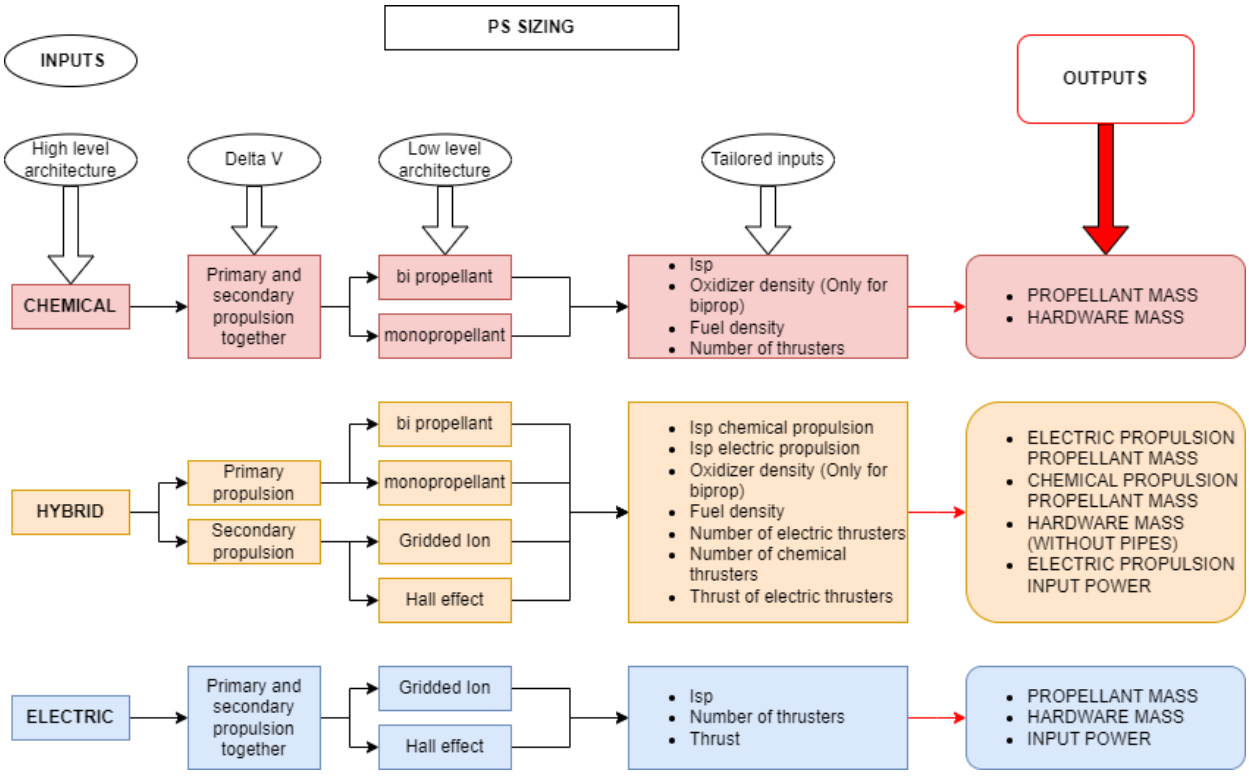

Figure 2.3: PS subsystems alternatives tree and inputs

ΔV values, based on the high-level choices provided as input. The outputs of the electrical and chemical propulsion system sizings are combined if hybrid propulsion is chosen. The underlying assumption for hybrid propulsion is that the transfer ΔV is assigned to the chemical thruster, while the station-keeping and, if applicable, the attitude ΔV budgets are allocated to the electric thrusters. This is in general true for communication satellites, but the situation changes for IOS satellites, which could perform an electrical orbit raising, but utilize chemical thrusters for the proximity operation. So a second hybrid propulsion option is inserted, that takes into account this difference. The equations utilized, referenced from [64], along with the architectural assumptions, will be presented in the following sections.

Bi-propellant chemical propulsion

The first equation of the system sizing is the well known Tsiolkovsky equation, that will then be used for every propulsion type for the evaluation of the propellant mass.

$$M_{prop} = M_{dry} \cdot (exp(\frac{\Delta V}{I_{sp} \cdot g_0}) - 1) \tag{2.7}$$

Here $g0 = 9.81 m/s^2$ is the acceleration constant, while the ΔV is given in input by the user, together with the specific impulse, I_{sp} expressed in seconds, of the thruster chosen. The densities of the fuel and of the oxidizer, named respectively ρ_{FU} and ρ_{OX} [7], are given in input by the user in kg/m^3 and are used to define the oxidizer to fuel ratio O/F and to evaluate the respective masses and volumes of fuel, M_{FU} and V_{FU} and of the oxidizer, M_{OX} and V_{OX}.

$$M_{FU} = \frac{M_{prop}}{1 + O/F} \tag{2.8}$$

$$M_{OX} = M_{prop} - M_{FU} \tag{2.9}$$

$$V_{FU} = \frac{M_{FU}}{\rho_{FU}} \tag{2.10}$$

$$V_{OX} = \frac{M_{OX}}{\rho_{OX}} \tag{2.11}$$

The volume of the tanks is obviously driven by the oxidizer and fuel volume already evaluated, and the shape of the tanks is considered to be spherical for an equally distributed pressure. From these 2 instances, one can retrieve the oxidizer and fuel tank radius, r_{tankFU} and similarly r_{tankOX}.

$$r_{tankFU} = (\frac{3 \cdot V_{FU}}{4 \cdot \pi})^{1/3} \tag{2.12}$$

The following step is the tanks' sizing. For the tank, Titanium is chosen as the reference material, due to its widespread presence referenced in the past geostationary platforms. Its higher performances with respect to Aluminum, in terms of density and robustness, make it the best choice, nevertheless the higher price. The burst pressure of Titanium, is $\sigma_{Ti} = 950 MPa$ and its density is $\rho_{Ti} = 4429 kg/m^3$. The average pressure tank is considered to be $P_{tank} = 3 MPa$. The data reported are referenced in [64]. As a consequence, the fuel tank thickness and mass are evaluated. The same equations are used for the oxidizer.

$$t_{tankFU} = \frac{P_{tank} \cdot r_{tankFU}}{2 \cdot \sigma_{Ti}} \tag{2.13}$$

$$M_{tankFU} = \rho_{Ti} \cdot 4/3 \cdot \pi \cdot ((r_{tankFU} + t_{tankFU})^3 - r_{tankFU}^3) \tag{2.14}$$

The pressurization gas used is Helium, due to its stable nature and its wide historical use and the gas behaviour is considered ideal. The gas specific constant is $R_{spec} = 2077.35 J/(kgK)$, the average tank pressure is $T_{tank} = 293 K$. The final pressure value is the tank fuel and oxidizer tank average value, $P_{pressF} = P_{tank}$, while the initial pressure

value is 10 times the final one, $P_{pressI} = 10P_{pressF}$ [64]. Then the mass of the pressurization gas is found, considering the entire fuel and oxidizer volumes together as V_{prop}, and the ideal gas law is used.

$$M_{press} = \frac{P_{tank} \cdot V_{prop}}{R_{spec} T_{tank}} \cdot \frac{1}{1 - P_{pressF}/P_{pressI}} \tag{2.15}$$

Then equations 2.12, 2.13 and 2.14 are used to evaluate the pressurizer tank mass. The masses of the tanks are then summed to report the hardware mass of the PS subsystem, while the pressurizer mass is added to the oxidizer mass and to the fuel mass to show the final propellant mass as a whole. In this sizing, the thruster masses and powers are neglected, because they do not have a relevant weight in the overall budgeting and would represent 2 more inputs in the overall algorithm. The mass of the pipes is also neglected, because wrong considerations can be made without knowing the actual configuration and volume of the satellite.

Mono-propellant chemical propulsion

For the monopropellant propulsion system sizing, as previously said, the only change is in the pressurization system. The engineering reasons to choose a monopropellant over a bi-propellant system for a GTO to GEO transfer maneuver, given its lower performances in terms of thrust and Isp, can be justified by the request for a lower complexity system, with high reliability. So, a blowdown system is more suited for the scope with respect to the fully regulated pressurization system.
The only change, with respect to the previous case, lies in the pressurizer mass evaluation and the simplifying assumptions and equation will be now reported. The main assumptions are on the blowdown ratio, $B = 6$, on the combustion chamber pressure, $P_{chamb} = 1MPa$, on the feeding line pressure losses, $\Delta P_{feed} = 50kPa$ and on the injection losses, $\Delta P_{inj} = 0.3P_{chamb}$. The cited assumptions are all referenced in [64], then the system engineer can be free to adjust those hypotheses, if more accurate information is available. The tank initial and final pressures are then evaluated.

$$P_{tankF} = P_{chamb} + \Delta P_{inj} + \Delta P_{feed} \tag{2.16}$$

$$P_{tankI} = B \cdot P_{tankF} \tag{2.17}$$

The set of equations to evaluate the propellant volume, is the same as above, so equations 2.7 and 2.10. Once the propellant volume is known, the initial gas volume must be

evaluated, with the use of the blowdown ratio.

$$V_{gasI} = \frac{V_{prop}}{B-1} \tag{2.18}$$

The pressurizer mass can now be retrieved with the ideal gas law, using the same assumptions for the temperature and for the gas specific constant of the previous section.

$$M_{press} = \frac{P_{tankI} \cdot V_{gasI}}{R_{spec} \cdot T_{tank}} \tag{2.19}$$

The tank volume is here evaluated as the sum of the volumes of the fuel and of the pressurizer and equations 2.12, 2.13 and 2.14 are implemented to find the final mass budget of the subsystem.

Electric Propulsion

For the Electric propulsion sizing the main assumption is based upon the use of Xenon as the propellant of the system, because it is the most widely used in literature and to avoid adding the working conditions of the gas as additional input to the user. These inputs would require a hypothesis on the typical temperature of the spacecraft tanks and a simulation of the gas state evolution, based on standardized information from National Institute of Standards and Technology (NIST) [36]. Instead, the analysis of Xenon isocore transformation [36], to evaluate its density and its pressure to remain in a supercritical condition are here previously evaluated, bringing to the following conditions: average density, $\rho_{Xe} = 1155 kg/m^3$ at $P_{tank} = 18.6 MPa$, these data are also referenced in [42].
Given this data and the input information from the user on the I_{sp} and on the ΔV, the propellant mass and the tank mass are evaluated with the equations 2.7, 2.10, 2.12, 2.13 and 2.14.
Differently from before, here the power input to the thrusters cannot be ignored and is evaluated with the following equation.

$$P_{thrust} = \frac{N_{thrust} \cdot T \cdot g_0}{2 \cdot \eta} \tag{2.20}$$

Where, N_{thrust} is the number of electric thruster operated simultaneously, T is the thrust generated by the single selected thruster and related to the I_{sp}. These quantities are all inserted in input by the user. η is the thruster efficiency and is considered to be 0.5 for the Hall Effect Ion thruster and 0.7 for the Gridded Ion solution [9, 18, 23, 30, 50–52, 54].
The mass of the Power Processing Unit (PPU) is evaluated with the use of the PPU specific mass parameter, which is considered to be $M_{spec} = 0.005 kg/W$ for the Hall effect

and $M_{spec} = 0.01 kg/W$ for the gridded ion [8, 18, 31, 40, 53].

$$M_{PPU} = P_{thrust} \cdot M_{spec} \tag{2.21}$$

The data are then summed to obtain the hardware mass and propulsion mass of the subsystem.

Hybrid propulsion

In case hybrid propulsion is selected by the user, the underlying need is probably because one of the 2 propulsion systems must be used for the GTO to GEO transfer. As a consequence, the dry mass in input to the Tsiolkovsky equation 2.7, is not anymore the dry mass of the spacecraft, but it must be the dry mass plus the propellant utilized for on orbit operations. As a consequence, there is the need to specify which type of propulsion is utilized for the GTO to GEO transfer, to add the propellant of the other subsystem to the dry mass. It must be also specified the type of chemical and electric propulsion, and 2 different ΔVs will be given in input, one for the chemical propulsion and one for the electrical propulsion. The resulting subsystem will have 2 separated set of tanks. The equations used have already been shown.

2.4.2. EPS

For the EPS subsystem, due to the Earth orbiting nature of the satellites selected, the solution upon which the subsystem is sized, is composed by solar panels for daylight operations and batteries for the eclipse phases. GaAs solar cells and Li-Ion batteries are chosen due to their higher performances with respect to the other options and to their large use in the industry nowadays. These are the state-of-the-art solution for the vast majority of the spacecraft platform in use nowadays, based on the variety of platforms selected for this study[33, 38, 39, 58, 59].
The restriction of the analysis due to the type of orbit selected, brings also to fixed values for other degrees of freedom, which can become parameters in case the orbit selected is changed for a further development of the tool. The constant values derived from orbital considerations are the following:

- Eclipse duration, $T_e = 4320 s$.
- Daylight duration, $T_d = 82223 s$.
- Sun ray incidence with respect to the panel, $\Theta = 23.44 deg$.

- Sun irradiance, $I_0 = 1366.1 W/m^2$.

The main input required by the sizing is the peak power of the satellite, but it could be used only for the sizing of the solar panels or a special battery pack could be sized in order to fulfill only the peak power application, if the duration is not too much. Here, instead, for a robust and oversized design, the choice has been made to use the peak power as both daylight power and eclipse power, in order to size both panels and batteries. As explained above, the peak power mode in this model can be or the nominal mode in which the payload is in use, or the transfer mode for GTO to GEO orbit raising, if the power requested by the electric propulsion in this phase is higher than the payload power.
The set of relations used for the sizing of this subsystem are taken from [64] and the workflow is hereafter reported.

$$P_{SA} = P_{peak} \cdot (\frac{T_e}{X_e \cdot T_d} + \frac{1}{X_d}) \tag{2.22}$$

Where, P_{SA} is the power requested to the solar panels, P_{peak} is the peak power and X_e and X_d are respectively the line efficiency of the power production in eclipse and in daylight. Direct Energy Transfer type of power management technique, with respect to Peak Power Transfer technique, has been chosen due to literature considerations on GEO satellites[28]. This led to fixed values for the 2 efficiencies, $X_e = 0.65$ and $X_d = 0.85$[28].

$$P_0 = \epsilon_{BOL} \cdot I_0 \tag{2.23}$$

P_0 represents the reference power per unit surface produced by the panel, and $\epsilon_{BOL} = 0.3$ [28] is the efficiency of the GaAs solar panel in this model used.

$$P_{BOL} = P_0 \cdot I_d \tag{2.24}$$

P_{BOL} is the power per unit surface produced by the panel at the beginning of its life. In the formula, $I_d = 0.77$[28] is the inherent degradation factor of the cells and takes into account production impurities and uncertainties.

$$L_d = (1 - dpy)^{lifetime} \tag{2.25}$$

Here L_d is the lifetime degradation of the panel due to the aging, $dpy = 0.0375$ [64] is the degradation per year of GaAs solar cells and $lifetime$ is the lifetime of the satellite expressed in years and is one of the main inputs of the mission.

Hereafter, the power density of the panel at the end of life is retrieved.

$$P_{EOL} = P_{BOL} \cdot L_d \tag{2.26}$$

Finally, the solar array total area is retrieved, without taking into account the needed voltage, which would have added another degree of freedom and of complexity to the model.

$$A_{SA} = \frac{P_{SA}}{P_{EOL}} \tag{2.27}$$

The solar array area is expressed in m^2. To retrieve the solar array total mass, a surface density of $\rho_{SA} = 6kg/m^2$ is retrieved [46], with the hypothesis of an Al 3003 honeycomb panel of 2 cm thickness.

$$M_{SA} = A_{SA} \cdot \rho_{SA} \tag{2.28}$$

For the batteries sizing, 2 important parameters must be introduced, the depth of discharge, $DoD = 0.8$, where the value selected is valid for GEO satellites [28], and the Li-Ion battery density, $E_m = 175Wh/kg$ [64]. Another assumption that has been made is about the recharging time, T_r which is assumed equal to the eclipse time, T_e. Hereafter, the battery sizing is reported.

$$C = \frac{T_r \cdot P_{peak}}{DoD \cdot X_e} \tag{2.29}$$

Where C is the required capacity of the battery in Wh and T_r is expressed in hours.

$$M_{batt} = \frac{C}{E_m} \tag{2.30}$$

The mass of the batteries is expressed in kg and the total mass of the subsystem can therefore be obtained.

$$M_{EPS} = M_{SA} + M_{batt} \tag{2.31}$$

2.4.3. Statistical sizing

The remaining subsystems are modeled using constant statistical values or linear regressions, depending on the specific subsystem. The TTMTC (separated from the communication payload in communication satellites in the present model) and TCS subsystems are modeled using constant statistical values. The assumption here is that the primary drivers behind the masses and powers of these subsystems are linked to orbital considerations. Once the orbit is defined, in this case, the Geostationary orbit, the external heat loads and eclipse cycles are also defined. Additionally, the main type and dimensions of

the antenna dishes, along with the power requested by the Telecom subsystem at a given streaming data rate, are determined. Therefore, the thermal control strategy remains common among different satellites, with changes in mass and power made for specific applications due to specific thermal constraints of the battery and other unknown payloads that are not significant for the scope of this work. Moreover, assuming that the dimensions of all housekeeping and telemetry data do not differ significantly between different satellites, the power of the TTMTC subsystem can also be considered unchanged.

On the other hand, the other subsystems, along with the harness mass and power charging and distribution, can be modeled as a statistical percentage of the dry mass and power of the spacecraft. The structure grows with the dry mass of the spacecraft, as the definition of the structural function itself is influenced by higher masses of internal components, leading to higher static and dynamic loads that must be sustained, resulting in a higher mass of the spacecraft structure. Similarly, the ADCS grows in both power and mass due to the change in the spacecraft's inertial properties that must be controlled with the higher mass, even if the mass and power of the attitude determination devices remain unchanged as the dimensions grow. The underlying assumption is that most spacecraft in GEO orbit utilize a 3-axis stabilization technique with the use of reaction wheels, which must be larger. The OBDH subsystem, on the other hand, grows with the dry mass and power of the spacecraft because higher masses and power are linked to a greater number of electrical components and the need for more channels and higher data dimensions due to monitoring more parameters. This is also associated with the need for more memory and computing power with higher mass and power needed by the processing unit. The power charging and regulation grow with the total power, due to the higher energy dispersion linked to higher power and a greater number of devices powered by the system. Lastly, the harness mass grows with the mass, for the same considerations made for the OBDH system, leading to more cables for both power and information channels.

TTMTC and TCS

To find the constant statistical values, a lot of difficulties have been encountered to find complete budgets of the spacecrafts. Two of the most complete databases on GEO satellites have been created by MediaGlobe[62] and in the SMAD book [64] and are here used, without taking into account the possible changes due to technology advancement. The datasets are reported in the Tables 2.2, 2.3 and 2.4.

The main issue with the dataset in Table 2.2 stays in the range of dry masses covered by the dataset, that does not take in consideration all the cases covered by this work. This can be a source of error for the validation part, but due to the underlying hypotheses so

Table 2.2: GEO satellite subsystems mass distribution [62]. All the values in the table are percentages, except for the dry mass.

Name	P/L	Struct	TCS	Power	TTMTC	ADCS	PS	$M_{dry}(kg)$
ANIK E	27.6	22.8	4.7	28.7	2.9	3.9	9.4	1270
Arabsat	21.4	15.8	5.3	30.9	5.1	11.6	10.0	573
Astra 1B	30.0	16.2	4.5	30.7	2.3	6.2	10.2	1179
Kopernikus	24.1	18.4	4.1	30.8	4.4	7.2	11.0	656
Fordsat	28.9	19.5	5.0	33.2	0.9	7.4	5.1	1094
HS 601	49.8	12.2	3.1	19.3	4.7	4.4	6.5	1459
Intelsat VII	30.8	17.3	6.7	25.8	1.0	10.1	7.6	1450
Intelsat VIIA	28.8	15.4	6.9	27.4	0.9	9.1	7.5	1823
OLYMPUS	28.5	21.6	5.2	27.4	3.0	5.2	9.2	1158
SATCOM K3	19.0	17.6	4.4	35.6	3.5	6.7	13.2	1018
TELSTAR 4	24.1	10.9	5.6	35.0	4.8	4.4	6.2	1621
Average	**28.4**	**17.1**	**5.0**	**29.5**	**3.1**	**6.9**	**8.7**	
STD Dev	**8.0**	**3.6**	**1.1**	**4.6**	**1.6**	**2.5**	**2.4**	

Table 2.3: GEO satellite subsystems mass distribution from SMAD [64]. All the values in the table are percentages, except for the dry mass.

Name	P/L	Struct	TCS	Power	TTMTC	ADCS	PS	$M_{dry}(kg)$
FLTSATCOM 1-5	26.54	19.26	1.75	38.53	2.98	7.01	3.94	849.6
FLTSATCOM 6	26.38	18.66	1.99	39.39	2.99	6.77	3.83	870.9
FLTSATCOM 7-8	32.80	20.80	2.14	32.75	2.50	5.68	3.34	1041.9
DSCS II	23.02	23.50	2.77	29.32	6.97	11.46	2.96	475.9
DSCS III	32.34	18.18	5.56	27.41	7.23	4.35	4.09	867.3
NATO III	22.12	19.29	6.51	34.74	7.51	6.33	2.43	320.4
INTELSAT IV	31.24	22.31	5.14	26.49	4.30	7.41	3.14	532.8
INTELSAT V	28.85	21.21	3.21	22.44	3.45	9.00	11.84	835.0
INTELSAT VI	37.60	17.94	3.08	25.40	4.74	4.14	7.10	1779.0
TDRSS	24.56	28.03	2.78	26.36	4.07	6.17	6.92	1565.7
GPS Blk 1	20.49	19.85	8.70	35.77	5.84	6.16	3.61	479.1
GPS Blk 2, 1	20.15	25.13	9.86	30.97	5.20	5.41	3.29	699.1
GPS Blk 2, 2	23.02	25.37	11.03	29.44	3.10	5.25	2.68	858.0
P80-1	41.06	19.00	2.35	19.92	5.21	6.33	6.13	1704.4
DSP 15	36.91	22.53	0.48	26.94	3.84	5.51	2.23	2114.9
DMSP 5D-2	29.85	15.63	2.79	21.48	2.46	3.07	7.42	814.6
DMSP 5D-3	30.45	18.41	2.87	28.97	2.02	2.92	8.66	1012.3
Average	**28.7**	**20.9**	**4.3**	**29.2**	**4.4**	**6.1**	**4.9**	
STD Dev	**6.2**	**3.2**	**3.1**	**5.6**	**1.7**	**2.1**	**2.7**	

Table 2.4: GEO satellite subsystems power distribution [62]. All the values in the table are percentages, except for the total power.

Name	P/L	TTMTC	ADCS	TCS	PS	$P_{G\&D}$	P_{CHARG}	$P_{tot}(W)$
ANIK E	86.2	1.2	0.8	2.9	NA	0.7	8.2	3482
Arabsat	72.7	2.8	9.2	6.7	NA	1.3	7.3	1362
Astra 1B	76.6	1.5	1.0	3.8	NA	2.4	14.7	2790
Kopernikus	63.5	2.0	2.8	16.6	NA	3.3	11.9	1412
Fordsat	79.1	1.7	4.2	3.0	NA	1.3	10.8	3110
HS 601	79.4	2.4	2.1	8.4	NA	0.9	6.9	3350
Intelsat VII	72.3	1.1	6.3	7.4	0.2	2.3	10.5	3569
Intelsat VIIA	79.1	0.6	5.0	4.9	0.1	1.2	9.2	4567
OLYMPUS	75.9	1.6	4.1	10.1	NA	1.2	7.1	2832
SATCOM K3	81.6	1.4	0.9	3.0	0.0	1.6	11.5	3150
TELSTAR 4	84.9	1.7	1.3	2.4	NA	0.7	8.9	5673
Average	**77.4**	**1.6**	**3.4**	**6.3**	**0.2**	**1.5**	**9.7**	
STD Dev	**6.37**	**0.61**	**2.66**	**4.29**	**0.09**	**0.81**	**2.42**	

far cited, the dataset is valid for the scope of the work. With the use of the information in the tables, the constant mass and power of the selected subsystems is retrieved and reported as the sum of the average value and the standard deviation, to cover the entire cases with an error which is oversized. However, both Tables 2.2 and 2.3 were used to retrieve the mass information of the subsystems and only the Table 2.4 was used for the power of the subsystems, leading to a more uncertain value for the subsystems power with respect to the mass.

$$M_{TCS} = 100kg \tag{2.32}$$

$$P_{TCS} = 75.6W \tag{2.33}$$

$$M_{TT\&C} = 75kg \tag{2.34}$$

$$P_{TT\&C} = 99.6W \tag{2.35}$$

ADCS, OBDH and Structure

As shown in the chart 1.1, the Structure, ADCS and OBDH subsystems and the harness mass and the charging and regulation power are linked to the dry mass and total power of the spacecraft with the use of statistical relations. These relations are taken from [34], with the use of a dataset of more than 400 satellites, so they are more reliable than the statistic constant values already shown. In particular, the equations employed for the

mass sizing are:

$$M_{ADCS} = M_{dry} \cdot 0.053 \tag{2.36}$$

$$M_{OBDH} = M_{dry} \cdot 0.0307 \tag{2.37}$$

$$M_{STRUCT} = M_{dry} \cdot 0.2441 \tag{2.38}$$

$$M_{harness} = M_{dry} \cdot 0.07 \tag{2.39}$$

In particular, the relation on the harness mass was not retrieved from [34], but from [64], due to the lack of harness information in the first reference. For the power sizing, the total power referred to in [34], was interpreted as the total power of the satellite bus, due to lack of further specification. The equation for the power sizing are:

$$P_{ADCS} = P_{bus} \cdot 0.126 \tag{2.40}$$

$$P_{OBDH} = P_{bus} \cdot 0.071 \tag{2.41}$$

The non-auxiliary relation were chosen due to the willingness to have covered the majority of the possible cases.

$$P_{Charging} = P_{bus} \cdot 0.5 \tag{2.42}$$

The charging and regulation power was instead retrieved from the Mediaglobe dataset, due to lack of data in [34].

2.5. Margin philosophy

The adopted margin philosophy generally follows a reference document [17], from European Space Agency (ESA). The margins used are explicitly reported here and are in accordance with European Cooperation for Space Standardization (ECSS) documents [15]. These margins are typically employed in the design of space missions, allowing for easy comparison with traditional non-automated design techniques. The margins adopted primarily pertain to the propulsion subsystem sizing. The first margins are applied directly after the inputs inserted by the user. Therefore, the ΔV inputs are intended without

margins.

$$\Delta V_{trans} = \Delta V_{transIN} \cdot 1.05 \tag{2.43}$$

$$\Delta V_{sk} = \Delta V_{skIN} \cdot 2 \tag{2.44}$$

Where ΔV_{trans} is obtained by then sum of the results of the simulated transfer maneuvers performed by the satellites and ΔV_{sk}, refers to the station keeping and attitude maneuvers, but refers in general to stochastic maneuvers or to maneuvers linked with high uncertainties. However, the margin on the station keeping will be omitted for the validation of the communication satellites, due to the high level of confidence related to the North-South station keeping ΔV in GEO. The dry mass used in input to the Tsiolkovsky equation is also margined, then the margin is also applied to the entire dry mass for the total budget.

$$M_{dryMAR} = M_{dry} \cdot 1.2 \tag{2.45}$$

A margin that takes into account the eventual propellant residuals is inserted for the propellant mass.

$$M_{propMAR} = M_{prop} \cdot 1.02 \tag{2.46}$$

Specifically for the electric propulsion, the entire propellant volume is margined.

$$V_{EPpropMAR} = V_{EPprop} \cdot 1.05 \tag{2.47}$$

While, for the chemical propulsion, a higher margin is considered.

$$V_{CPpropMAR} = V_{CPprop} \cdot 1.1 \tag{2.48}$$

In addition, for the chemical propulsion, a margin on the pressurizer mass is considered.

$$M_{pressMAR} = M_{press} \cdot 1.2 \tag{2.49}$$

To conclude, for the electric propulsion, a 10% margin is considered for the PPU mass, due to a finer sizing that will result at the end of the spacecraft design for the choice of actual existing PPUs.

$$M_{ppuMAR} = M_{ppu} \cdot 1.1 \tag{2.50}$$

However, no margin has been adopted for the peak power budget because the peak power

given as output is referred to the total power produced by the solar array, shown in equation 2.22, so it already presents a growth from its original value. In addition, the statistical design part does not use as reference the designed data of the spacecraft, but the real ones. So these data are already margined and a further margin, would lead to an unreal result. So, the final choice is left to the user whether to utilize a further margin on the total mass and at which extent.

3 | Validation

The tool underwent validation using two distinct datasets comprising communication satellites, as accurate information regarding IOS satellites in GEO was unavailable. Two separate validations were conducted: one for chemical and hybrid design and another for all-electric satellite design. A comparison was also performed with the statistical relations presented in [41] for all-electric satellites and with the SDM in [34] for chemical and hybrid propulsion satellites.

The primary challenge encountered was related to the estimation of payload mass and power due to the proprietary nature of this information. Payload characteristics significantly influence the satellite sizing, introducing uncertainties if not accurately known. In [2], the payload masses are explicitly provided. For other satellites in the test, information was obtained using the statistical relation in Figure 1.1, linking the number of transponders to payload mass, and a model extrapolated from the sizing of communication payloads in the SMAD book[64] for payload power. The age of the book could introduce errors, potentially affecting the tool's validity.

A further proof for the tool, consists in comparing the results of the first statistical relation with the tool, inside the frame of communication satellite part of the dataset utilized by the models and the tool can be considered validated because as shown from the Figures 3.1 and 3.4, the error of the tool is similar or lower.

In the second phase of validation, the tool's flexibility was demonstrated by comparing its output with a pool of satellites used for meteorology, navigation, or scientific purposes, which had characteristics external to the database. The output data were marginally adjusted using a 20% margin for dry mass, as explained in the previous chapter, and the total power shown represented the power produced by the solar panels, considering line losses under the hypothesis of Direct Energy Transfer architecture design.

The relative error, expressed as a percentage, was calculated as the absolute value of the difference between the computed quantity (Q_{comp}) and the real quantity (Q_{real}) divided by Q_{real} and multiplied by 100.

$$Err_{rel} = \frac{|\mathrm{Q}_{comp} - \mathrm{Q}_{real}|}{\mathrm{Q}_{real}} \cdot 100 \tag{3.1}$$

This approach was employed for both power and mass errors. The results demonstrated the tool's capabilities, and the validation was separated between chemical and all-electric satellites to showcase the tool's effectiveness.

3.1. Chemical and hybrid satellites

For the validation of chemical satellites, statistical relations from [34] have been employed. This choice is justified by the fact that, between 2000 and 2018, the majority of GEO-launched spacecraft were chemical satellites, making them a suitable candidate for comparison. Additionally, the initial iteration of the tool relies on some of the same relations. Therefore, superior performance in this validation indicates the accuracy of the assumptions, sizings, and relations for satellite subsystems.

The set of validating relations, denoted as "FADSAT SDM" comprises the equations previously introduced: 2.1 for total mass, 2.2 for dry mass, and 2.3 for total power. It is essential to note that this leads to a greater uncertainty in total power compared to total mass due to error propagation. The only modification is in equation 2.3, where the focus is on total power rather than bus power. Consequently, the assumption of a 25% power allocation for the bus power is omitted, and the relation simplifies to:

$$P_{tot} = M_{dry} \cdot 4.15 - 1665 \tag{3.2}$$

In contrast to the "GEOdesign tool," the key distinction lies in the input requirements. Here, only the satellite payload mass is needed, while the latter tool demands both payload power and additional inputs crucial for system engineer trade-offs, aligning with the primary objectives of this work. The rationale for this divergence is the uncertainty associated with satellite payload power, rendering a statistical relation less reliable. Consequently, the payload power is initially associated with the total mass, and then the total mass is linked to the total power. These quantities are generally well-documented and widely available, as referenced in [16, 25, 60, 63].

3.1.1. Input

In this section, the primary inputs chosen for the satellite design, used for validation, will be presented and justified.

Payload Mass

To align with the statistical relations utilized for validation, a combination of the relations shown in 1.1 is employed for communication satellites. The input for this relation is the number of transponders on the satellites, easily obtainable from sources such as [16, 25, 60, 63], and the output is the payload mass.

$$M_{pay} = \frac{N_oT \cdot 84 + 177}{11.9} \tag{3.3}$$

Here, N_oT represents the number of transponders. For non-communication satellites payload mass information was gathered from mission-related websites and, when unavailable, a similar payload's information was used. However, this process introduces a potential source of error for validation, as the primary factor driving satellite selection was the availability of payload information.

Payload Power

For payload power, two reference tables from [64] displaying power breakdowns for communication payloads were considered. The first table represents the power breakdown for a communication payload with 48 C-band transponders, and the second table represents 48 Ku-band transponders. Without replicating the entire power budget for each satellite, the final data on power consumption was considered, and a reference formula was derived.

$$P_{pay} = \frac{5690}{48} \cdot N_oT_{C-band} + \frac{11320}{48} \cdot N_oT_{Ku-band} \tag{3.4}$$

Two main simplifications introduce potential errors in the payload power estimation. First, the reference communication payload power breakdown includes the use of Travelling Wave Tube Amplifier (TWTA), which is less efficient than Solid State amplifier. Second, technological advancements were not considered, potentially leading to a reduction in power in the overall budget. For non-communication satellites, similar to payload mass, power characteristics were obtained from various websites, with the substitution of the power consumption of a similar payload when information was not available.

a_{GEO}	42164 km
a_{GTO}	24531 km
e_{GEO}	0
e_{GTO}	0.72
i_{GEO}	0°
i_{GTO} (Ariane 5)	7°
i_{GTO} (Falcon 9)	28.5°

Table 3.1: Orbital parameters of initial and final transfer orbits [7].

Delta V

The ΔV for the GTO to GEO transfer is obtained with the hypothesis of an Apogeo Kick maneuver, which consists in a single firing performed at the apogee of the Geostationary Transfer Orbit, in which both the circularization of the orbit and the plane change are executed. The formula for the apogeo kick is the Carnot Theorem, and is here reported [7]:

$$\Delta V_{transfer} = \sqrt{v_a^2 + v_{GEO}^2 - 2 \cdot v_{GEO} \cdot v_a \cdot cos(\Delta i)} \tag{3.5}$$

Where the initial and the final orbit have the parameters shown in Table 3.1. As a consequence, two different $\Delta V_{transfer}$s are obtained, one for the Falcon 9 GTO [61] with $\Delta V_{transfer} = 1800 m/s$ and one for the Ariane 5 GTO [5] with $\Delta V_{transfer} = 1500 m/s$, due to the difference in their inclinations. For the station keeping, instead a reference value of $55 m/s$ per year is considered [7], and this value is multiplied by the lifetime expressed in years, which is easy to find in the above cited websites.

Thruster and propellant characteristics

The chemical thrusters used for the apogeo kick, as seen from the most widely used buses Spacebus, Eurostar, SSL1300 and AS2100 [25, 33, 58, 59] have almost the same characteristics. A thrust around 400N, a specific impulse around 300s and are all bipropellant thrusters running on Monomethyl Hydrazine (MMH) as fuel and Nitrogen Tetroxide as oxidizer (N_2O_4). The reference densities for the propellants are $\rho_{MMH} = 880 kg/m^3$ and $\rho_{N_2O_4} = 1470 kg/m^3$ [28]. The thruster taken as references are the EADS Astrium S400, for the apogeo kick and the EADS Astrium S10 for the station keeping, because they can share a common tank system, but have different thrust ranges and are the reference propulsion system for the Spacebus 4000 series [58] for the chemical version. All the characteristics are described in the Table 3.2. As can be seen from the chamber pressure information, the hypothesis expressed in the section 2.4.1 and used inside the sizing, holds for both cases. However, the user is free to change this information if a precise thruster

Characteristic	EADS ST S10	EADS ST S400
Thrust	10 N	400 N
I_{sp}	290 s	318 s
Nominal chamber pressure	9 bar	10 bar

Table 3.2: EADS ST thrusters characteristics [21].

Thrust	0.115 N
I_{sp}	2000 s

Table 3.3: Fakel SPT 100 thruster characteristic, for $\eta = 0.5$ [9, 52].

sizing is needed.

For the hybrid satellites, for the primary propulsion design inputs EADS S400 is used also here, but for the secondary propulsion, the FAKEL SPT 100 D Hall effect thruster is used, which is a flight proven thruster used in the Eurostar 3000 satellite bus series [14, 43]. The propellant used is Xenon, which holds the hypothesis on the propellant characteristics utilized in the section 2.4.1. The electric thruster presents a usage curve, that varies thrust and specific impulse, based on the input power. Here, to hold the hypothesis on the efficiency done in section 2.4.1, which is 0.5 for the Hall Effect thrusters, the values of the curve corresponding to that efficiency are selected, which also correspond to the optimum values. The thruster characteristics in this way retrieved are reported in the Table 3.3.

3.1.2. Communication satellites

The inputs outlined in the preceding sections are utilized for the preliminary sizing of a pool of satellites used to validate the code for chemical and hybrid applications. The selected satellites include those used in [34] as a case study for the validation of the entire code, and additionally, some other communication satellites with hybrid propulsion launched from 2000 to 2018 and using satellite platforms included in the statistical dataset are chosen, as they are likely part of the dataset. In the second figure, the dataset's actual total masses and solar array powers are reported, while in the first one, the relative errors with those values are reported.

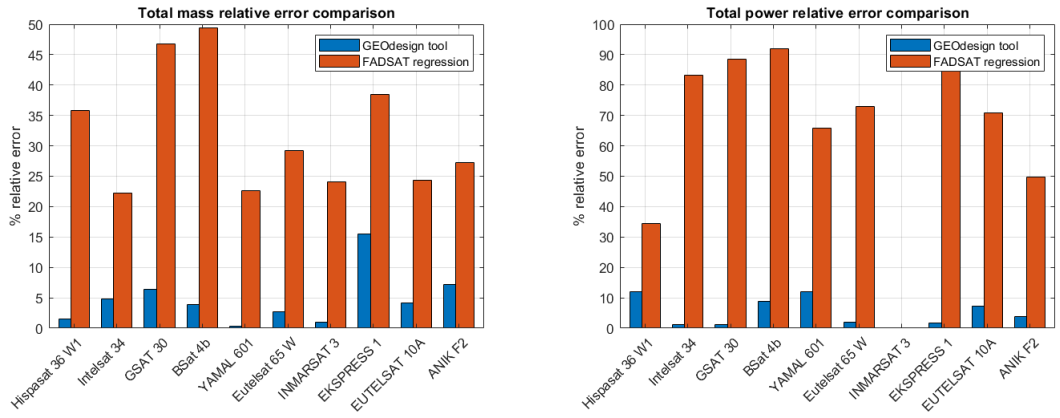

Figure 3.1: Relative error comparison on total mass (left) and on total power (right) for communication chemical and hybrid satellites.

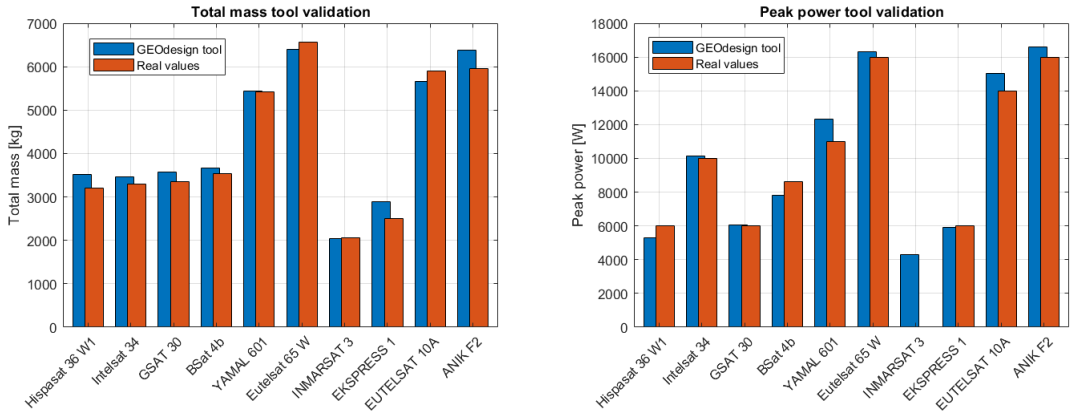

Figure 3.2: Total mass (left) and total power (right) comparison for communication chemical and hybrid satellites.

In Figure 3.2, it is evident that the tool is validated, as the values are similar to the real ones. However, slightly lower errors are generally obtained for the total mass budgeting than for the solar array power budgeting. In fact, the average relative error for the mass budget is 3% and 3.3% for the power budget. The standard deviations of the relative errors are, instead, 4.3% for the mass budget and 4.5% for the power budget, demonstrating the high precision for the sizing of communication mission architectures, due to the choice of communication satellites datasets for the statistical sizings. Higher reliability for the mass budgeting with respect to the power budgeting is also an evidence. This discrepancy is attributed to the uncertainty related to the payload power consumption, a major driver of the total power. The payload is the main contributor to the power budget due to the absence (for chemical satellites) or lower contribution (for hybrid satellites) of the electric

thrusters' power consumption, assuming that the thrusters and the payload are not used concurrently, as stated in the section 2.1.

The highest mass relative error of 15%, shown in Figure 3.1, is obtained for Ekspress AM1 satellite mass, whose value is at the boundary of the 3σ value of 15.9%. The reason is linked to the input payload mass of 95 kg, outside the dataset input limitations. The wrong input payload mass leads to an overestimation of the drymass and consequently to an overestimation of the entire mass of the satellite, despite the correctness of the solar arrays power. The highest power errors are obtained for the satellites Hispasat 36 W1 and YAMAL 601 whose relative errors are around 10%, due to the difference in the electric thrusters used as secondary propulsion, than the one used in input, and to the uncertainty on payload information. However, the errors are contained and acceptable for the scope of the work. Inmarsat 3 is reported because it is an interesting case, which makes the validation more robust, even if there is no information on the solar array power of the satellite, this is why the information is not reported in Figure 3.2. This is the only satellite in the test dataset, that does not perform an apogee boost maneuver, but is directly inserted in GEO. So, only the station keeping ΔV is inserted in the sizing, leading to a correct sizing like for the other cases.

3.1.3. Non communication satellites

The non communication satellites are compared to show the tool flexibility in operating outside the usual application in Geostationary orbit and to extend the validity of the hypotheses outside the statistical dataset from which are taken. If the tool gives acceptable results also in these applications, it means that is better than the actual possible methods for a preliminary sizing of a non communication satellites and is flexible enough for the preliminary design of a new concept satellite like the satellites for IOS. Here the tool is not compared anymore with the statistical relations utilized in the tool and regarding the communication GEO satellites, but is compared with several statistical relations, commonly used for the sizing of Earth orbiting satellites to highlight the importance of such tool. Those relations are:

- Zandbergen relation [47]:based on 34 data of Earth orbiting satellites.

$$M_{tot} = 3.66 \cdot M_{pay} \tag{3.6}$$

  It has a correlation coefficient of 0.899 and the payload input range is between 20 and 2150 kg.

- Brown relation for meteorological satellites[10]:based on 8 data points of meteorological satellites.

$$P_{tot} = 1.96 \cdot P_{pay} \tag{3.7}$$

  The payload input range is between 100 and 450 W.

- Brown relation[10]:based on 40 data points of Earth orbiting satellites.

$$P_{tot} = 1.13 \cdot P_{pay} + 122W \tag{3.8}$$

  It has a correlation coefficient of 0.899 and the payload input range is between 5 and 1000 W, and is used for the non-meteorological satellites.

- SMAD book relation for large satellites[64]:

$$P_{tot} = 1.85 \cdot P_{pay} \tag{3.9}$$

  Which is estimated to obtain relative errors around 35%.

So a further validation, with non communication satellites, is presented in Figure 3.3. The biggest issues regard the total power budget.

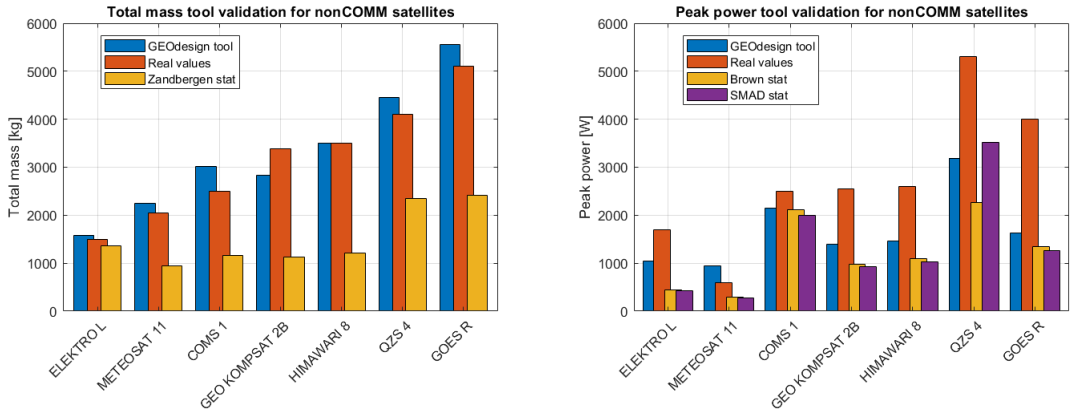

Figure 3.3: Total mass (left) and on total power (right) comparison for out of the database chemical and hybrid satellites.

As previously noted, the estimations are more accurate for the mass budget than for the power budget. This is likely due to uncertainties in both the payload and the power of the payload. The higher average error is a result of the statistical relations used being ill-suited for satellites with a different purpose, even if they share the same orbit. However, the results obtained are notably superior for total mass sizing when compared to

Zandbergen's statistical relation and marginally better than Brown's relation and SMAD relation for power. This reaffirms the tool's utility in comparison to the use of a common statistical relation. The average relative error of the tool lies around 15 % for the mass budget and 43 % for the power budget, with respective standard deviations of 9% and 15%. These data indicate the that sizing is 12% less accurate on average, with respect to communication satellites mass sizing, however it is still a very good result for the phase of design for which the tool is intended to be used, especially if compared with Zandbergen's relation results. There is also a good alignment with the 20 % design margin inserted in the dry mass. Significant errors are obtained by every relation in the power sizing, as depicted in Figure 3.3, the issue may lie in the underestimation of payload powers found online or in the total reference total powers of the satellites, whose data found are poor. This sentence is sustained by the fact that the average relative error obtained by the tool, which is in line with the error obtained by the SMAD relation, is 10% higher than the error expected by the SMAD book. A further analysis on the power error will be required for the future works. However, neither one of these satellites is of hybrid type. Therefore, the error is expected to be lower for hybrid propulsion satellites, because the influence of the power requested by the electric thrusters can become more important than the payload needs, leading to more accurate results.

3.2. All-electric satellites

The behaviour of the tool for the all-electric satellites test is separated from the validation on the chemical and hybrid satellites, because the statistical relations it is based on for the first iteration of the code are different, as explained in section 2.2. So, like in the previous chapter, the comparison relations are the ones used in the first iteration, so equation 2.5 for the total mass, and equation 2.6 for the total power, to be evaluated once obtained the total masses in the first equation. The difference is that the interest is not in the bus power but in the total power. The second equation becomes:

$$P_{tot} = (0.0034 \cdot M_{tot} + 0.9759) \cdot 1000 \tag{3.10}$$

The same considerations on the difficulties of finding the correct payload power hold also for this case and a possible error can be based on the uncertainty on the payload power information, that in this set of statistical relations is decoupled from the total power, while for our assumptions these quantities can be strictly related.

3.2.1. Input

In this section, the main inputs chosen for the satellited design used for the validation will be exposed and justified, with a little change on the input ΔV for the orbit raising with respect to the previous case.

Payload Mass

The payload mass, differently from before, is given in the dataset used as test case, which is the same of the statistical relations used and shown in [41]. Here, differently from the previous section, it has been impossible to find an all-electric satellite in GEO with non communication purposes. This enhances the need of this tool, but at the same time forced the flexibility of the electric side of the tool to be tested on a series of communication satellites, with the only peculiarity to be out of the dataset used in [41], so launched from 2018 to today. For these satellites, for coherence with the first validation, the payload mass is retrieved with the use of a statistical relation present in Figure 1.4, hereafter reported for completeness.

$$M_{pay} = 65.651 \cdot exp(0.0409 \cdot N_oT) \tag{3.11}$$

The input needed, as before, is the total number of transponders of the satellites, N_oT and the output is expressed in kg.

Payload Power

The payload power, for both the cases, is retrieved with the use of a statistical relation shown in Figure 1.4 and here reported for completeness.

$$P_{pay} = (3.6147 \cdot exp(0.0007 \cdot M_{pay})) \cdot 1000 \tag{3.12}$$

Where the result is expressed in W. Differently from before, here the communication payload breakdown developed in [64] is not used due to the presence of a more precise relation.

Delta V

The ΔV for the station keeping is defined as above with the little difference that the average ΔV needed per year is multiplied by the lifetime minus one, because one year is necessary to reach the GEO orbit in low thrust. For the $\Delta V_{transfer}$ a correction is

Characteristic	XIPS 25	PPS 5000	SPT 100 D
Thruster type	Gridded Ion	Hall Effect	Hall Effect
Thrust	0.165 N	0.3 N	0.112 N
I_{sp}	3550 s	2000 s	2000 s
Efficiency	70%	50%	50%

Table 3.4: Electric thrusters for orbit raising [9, 23, 50].

performed that takes into account the low thrust nature of the orbital transfer. A margin of 1.4 [22] is inserted to obtain the new $\Delta V_{transfer}$ needed for the electric propulsion. As a result, $2100 m/s$ is the input for satellites launched on a GTO with 7° of inclination and $2520 m/s$ is the input for satellites launched on a GTO with 28.5° of inclination.

Thruster and propellant characteristics

The spacecraft platforms for the all-electric satellite options ever launched in GEO include: BSS-702 SP (Boeing), LM2100 (Lockheed Martin), SSL 1300 (Space System Loral), Express 1000 HTP (ResHeTNev), Eurostar E3000EOR (Airbus), USP (RSC Energia), and Small GEO (OHB) [2]. It is known that SSL 1300 and E3000 EOR use Hall electric thrusters, specifically the BPT 4000 and PPS 5000 thrusters, respectively [43, 59]. BSS 702 SP, on the other hand, uses a gridded Ion thruster named XIPS 25 [41]. Therefore, for the sizing of satellites using Hall Effect thrusters are inserted in input the characteristics of PPS5000 or SPT 100 D, which is the most widely used in literature, even if mainly for orbital control [25]. The XIPS 25 characteristics are used for satellites utilizing gridded ion propulsion. The relevant characteristics are summarized in Table 3.4, corresponding to the efficiency used in the code. The propellant for all architectures is assumed to be Xenon, strengthening the assumption made in section 2.4.1. A case-by-case trade-off on the number of thrusters is made depending on the total mass of the satellite.

3.2.2. Communication satellites

In the previous section, the satellites tested for validation belong to the dataset of statistical relations utilized for the first iteration of the all-electric satellite sizing [41]. Unlike the chemical and hybrid propulsion case, the main driver of the peak power of the satellites in the all-electric case is electric propulsion, which is sized and would therefore lead to a lower level of uncertainty. This is not evident from the overall relative error on the solar array power shown in Figures 3.4 and 3.5, and it could be motivated by the presence of errors on information on the payload power furnished in [2].

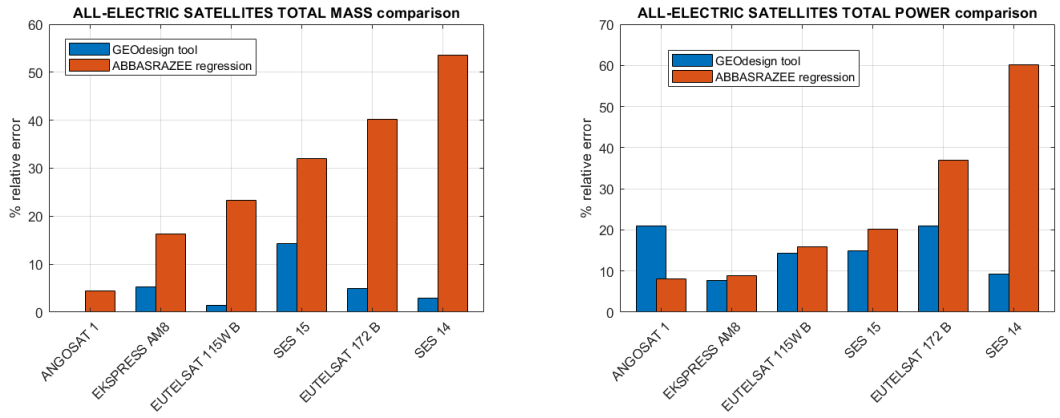

Figure 3.4: Relative error comparison on total mass (left) and on total power (right) for communication all-electric satellites.

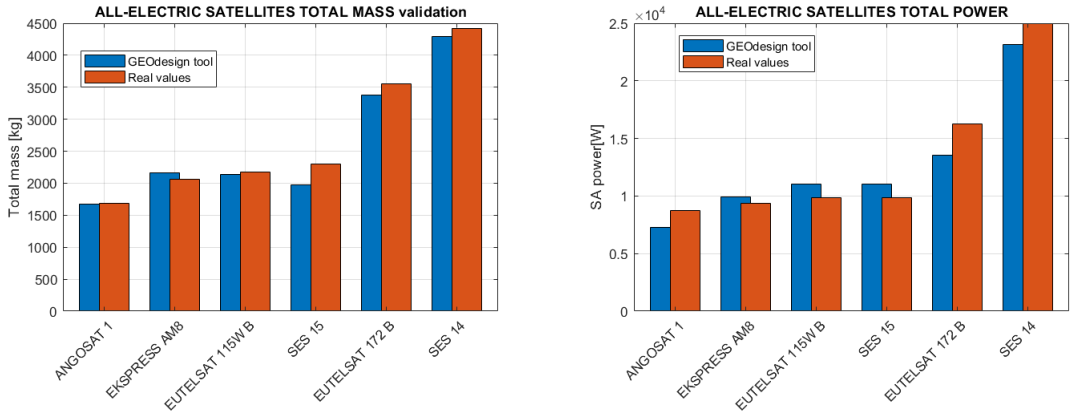

Figure 3.5: Validation on total mass (left) and on total power (right) for communication all-electric satellites.

In the figures shown, it is clear that the sizing of the electric propulsion system leads to slightly different results than before, and the average error is higher for both the budgets. A further reason may lie in the presence of a lower number of spacecrafts in the dataset used in [41], with respect to the datset used in [34], that links obviously to an error increase. However, the tool is validated also for this type of architecture, with relative errors that are lower or comparable to the set of statistical relations developed in [41]. The average relative errors obtained are around 5% for the total mass sizing and 15% for the total power sizing, with standard deviations around 5% and 6%. The low deviation standard in the power, is justified by the architecture type, in which the main driver of the budgeting is the electric thrusters power. So, once the electric thruster type and number is correctly chosen, the solar array power lies around that value for each designed

spacecraft, with peculiar differences given by the bus power, which is estimated from the payload mass. As a consequence, once again, the main driver in the error growth may be conducted to the uncertainties related to the input payload characteristics. The low relative errors obtained for the mass estimation are instead linked to the sizing of the propulsion system. With respect to the power estimation, here the correctness of the ΔV in input mitigates the effect of an inexact estimation of the dry mass of the satellite, which is linked to both the power error (difference in the weight of the solar panels) and to the payload mass error. This is also evident in the similar standard deviation with respect to the power estimation, which can only be linked to the error in the mass input The mitigation made by the PS sizing lowers the mass average error, while it highers the power average error, due to the limited set of thrusters and operating conditions used as inputs. For Angosat 1, as seen from Figure 3.4, the relative error is worse than with the use of statistical relations in [41] for the total power. The problem can be linked to the absence of knowledge of the thrusters used in the USP Bus used by Angosat 1 and to the number of thrusters used, leading to uncertainty on the total power. All the powers found in literature are multiplied by 1.25 to take into account the power produced by the solar array, where no explicit indication that the power reported is the power produced by the solar arrays, as is done for the output of the tool.

3.2.3. Out-of-Database Satellites

As previously mentioned, there are currently no all-electric satellites in GEO orbit designed for a purpose other than communication. This led to the use of all-electric communication satellites launched after 2018 that are out of the dataset selected for statistical relations. This allows us to examine the improvements brought by the tool when a satellite outside the dataset is selected.

In Figure 3.6, it is evident that the tool is more suitable than statistical relations for preliminary sizing. However, no visible trends can be extrapolated due to the low number of satellites in this category, but it is clear that the trends in terms of relative errors are the same of the previous case. However, it is not the same for the statistical relations found in [41], for which the relative error is visibly grown, when a satellite outside the dataset is selected. The average relative errors obtained are around 9% for the total mass sizing and 17% for the total power sizing, with standard deviations around 4% and 11%. The relative errors are higher than in the previous case, in line with the error growth of the statistical relations used for the first iterate. However, this first error is then mitigated by the mission analysis input and the propulsion system input. The standard deviation of the total mass is in line with the previous case. The standard deviation of the total power

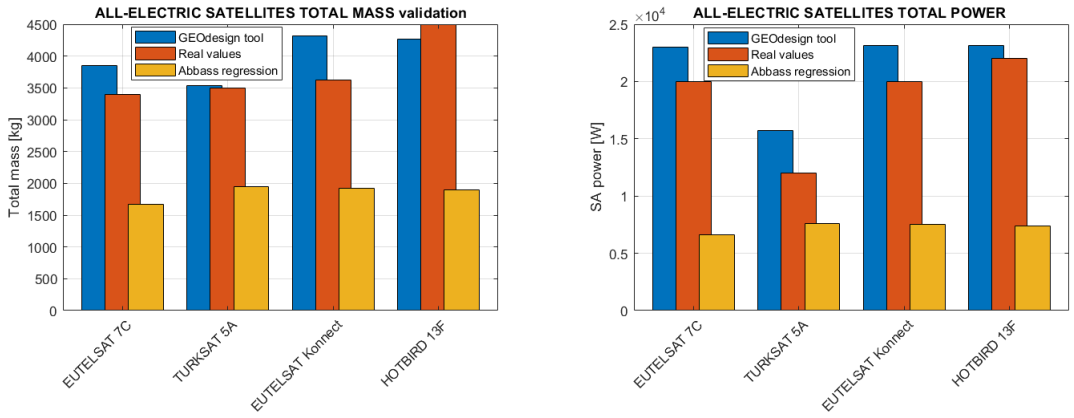

Figure 3.6: Total mass (left) and on total power (right) for out-of-database all-electric satellites.

is then due to the relative error of Turksat 5A, which is similar to the others in absolute value, but presents a lower value of the real budget, resulting in a growth in the standard deviation. The consistency of the error on the power budget, not the relative one, is due to the input characteristics of the thruster, as before, which can be tuned better if exact the operative information are known. It is a further proof of the flexibility of the tool for the preliminary sizing of new satellites.

4 | Case studies

After the validation of the tool, different practical cases of the preliminary sizing of IOS satellites are performed. The tool will be used to perform a trade-off on the type of propulsion selected, once the mission scenario is defined, and to look at the variation of the satellite's budgets due to the changes in the mission architecture. The two selected mission profiles and scenarios have been studied by National Astronautics and Space Administration (NASA) in [3], and the main features useful for the inputs' selection will be now described. At the end, the results obtained by the study will be compared to the tool output.

4.1. Mission scenario 1

The Notional Mission 1 (NM1) study [3] focuses on designing a Servicer spacecraft capable of capturing and controlling multiple legacy non-cooperative satellites in nearly co-planar geosynchronous orbits. The objective is to relocate these satellites, such as Solar Dynamics Observatory (SDO) and Geostationary Operational Environmental Satellite (GOES), to a disposal orbit 350 km above the GEO belt and acts as shown in Figure 4.1. The Customer satellites, assumed to tumble at 0.25 degrees per second per axis, are boosted using supervised autonomous rendezvous and capture, here denoted as Autonomous Rendezvous and Capture (AR&C), techniques. The Servicer, equipped with necessary hardware and fuel, executes sorties to approximately 10 Customer satellites, with about one degree of orbit plane change between each. The mission life spans 5 years, servicing 10 Customers.

4.1.1. Mission Details

- **Launch and Approach**: The Servicer is launched into geosynchronous orbit and gradually approaches the Customer satellite over 4.5 days, using co-elliptic drifts and Hohmann transfers. Once in proximity, it moves onto a safety ellipse around the Customer and collects situational awareness data.

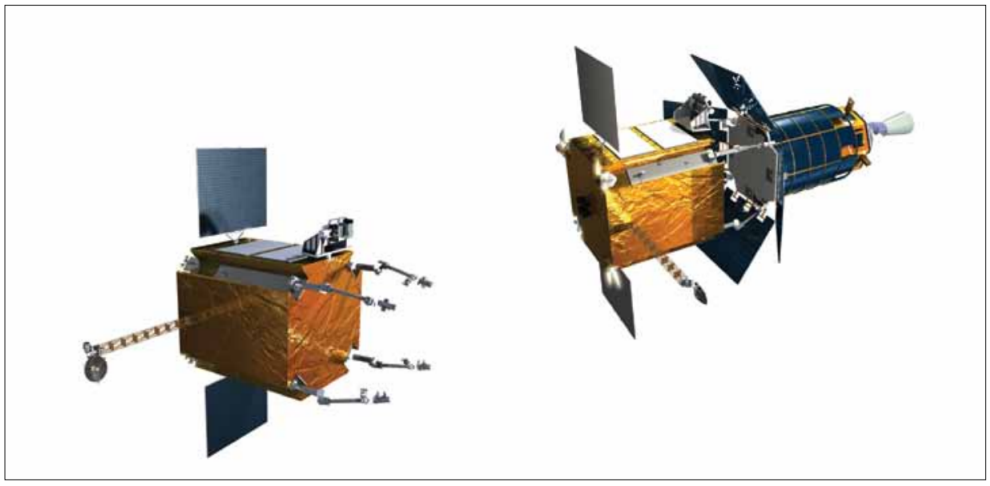

Figure 4.1: Servicer in Launch, Deployed and Docked Configuration (Credit: NASA).

- **Rendezvous and Capture**: After confirming safety, the Servicer executes maneuvers to approach the Customer along a straight-line path. Robotic arms autonomously grasp the Customer at predefined points, completing the capture. The Customer goes into free drift, and the Servicer controls the combined stack.
- **Disposal**: The Servicer boosts the stack into a super-synchronous disposal orbit (GEO + 350 km) following NASA guidelines for limiting orbital debris. After releasing the Customer satellite, the Servicer lowers itself to a parking orbit 300 km above GEO until the next Customer mission.
- **Mission Operations**: Operations are conducted from NASA's Goddard Space Flight Center's Servicing Mission Operations Center (SMOC). The AR&C phase is supervised from the ground, with scheduled hold points for assessments. Robotic activities are teleoperated post AR&C phase.

The summary of the phases and the ΔV budget needed to dispose the first satellite are shown in the Figure 4.2 and comprehend $11m/s$, to firstly reach the parking orbit and $48m/s$, for the remaining maneuvers to approach the target, capture, complete the disposal and come back to the parking orbit. These last operations can then be repeated for every customer, so $48m/s$ at least are needed per each customer satellite.

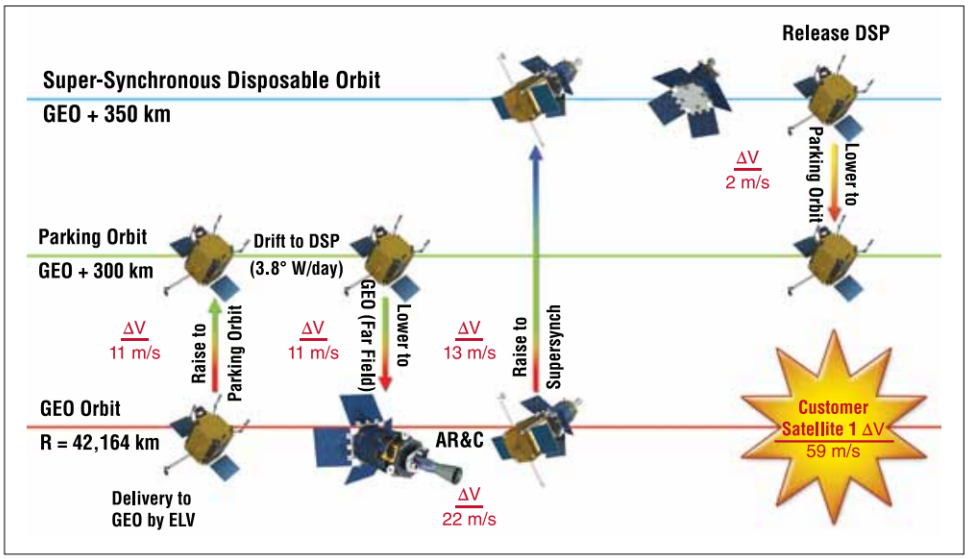

Figure 4.2: Orbital Maneuvers Performed during Customer Capture and Boost (Credit: NASA)

4.1.2. System description

The Servicer spacecraft design incorporates sensors, algorithms, and four robot arms for autonomous capture of non-cooperative Customer satellites in geosynchronous orbit, followed by boosting them to a disposal orbit. The AR&C package includes sensors and avionics, featuring a pan/tilt unit. The AR&Cpackage's total mass is 141.1 kg, with peak power draw at 128.9 W and peak data rate at 996 Mbps (786 Mbps with compression). The dimensions of the AR&C sensors and avionics package are 1400 × 750 × 723 mm.

The Servicer is equipped with four 2-meter robot arms, affixed to the front corners, capable of grasping the Customer spacecraft autonomously. During the AR&C phase, the arms hold the Customer as the Servicer boosts the stack. Each arm is attached via a mounting surface housing control avionics and is hard-mounted to the spacecraft structure. A gripper with Laser Imaging Detection and Ranging (LIDAR) senses the Customer, and arms are teleoperated from the ground except during AR&C phase, ensuring a signal latency of less than 3 seconds.

The Servicer features a 3-axis stabilized, sun-pointing, fully redundant bus system with deployable, gimbaled solar arrays mounted 180 degrees apart. The power system provides approximately 1,500 W of total average power and includes two 100 Ahr Li-Ion batteries. The system design utilizes chemical propulsion, with a dry mass of 2,352 kg (including 30% contingency) and a wet mass of 3,694 kg. It can be launched on an Atlas V with 7% margin or a Delta IV Heavy with 70% margin.

Integrated Design Laboratory Robot Arm

The Integrated Design Laboratory Robot Arm (IDL) Robot 1 is a dexterous robot system developed during the first Instrument Design Laboratory run, based on existing space robot systems—Ranger (developed by the University of Maryland's Space System Laboratory) and Front-end Robotics Enabling Near-term Demonstration (FREND) (developed by Alliance Spacesystems, now MDA, and the Naval Research Laboratory for DARPA). It is the robotic arm taken as reference for the devolpement of the explained mission. The 7-Degree of Freedom (DOF) notional arm has a 3-DOF shoulder, 2-DOF elbow, and a 2-DOF wrist, totaling approximately 2 meters in length and fitting within a 0.35 m^3 volume. The arm's weight, including electronics, is 157 kg, with 34 kg attributed to electronics. It operates at 380 W power and can transmit data at 1 Mbps. The specifications are summarized in 4.1.

Table 4.1: IDL Robot 1 Specifications [3]

DOF	7 (3-DOF shoulder, 2-DOF elbow, 2-DOF wrist)
Total Length	Approximately 2 meters (divided equally between upper and lower arm)
Volume	0.35 m^3
Total Weight	157 kg (electronics: 34 kg)
Power Consumption	380 W
Data Transmission	1 Mbps

The entire mission shown is summarized in the table 4.2.

4.1.3. Input

From 4.2, the main inputs are extrapolated. The assumption is that the payload here is considered to be composed by the devices that enable the servicing: the 4 Robotic arms and the AR&C sensor package. The ΔV is comprehensive of the budget needed for each customer and the station keeping maneuvers. The only characteristic known about the propulsion system is that it is fully chemical, so both monopropellant and bipropellant solutions will be analyzed, and then a trade-off with the electric propulsion will be made. However, in the next section, only the chemical propulsion solution will be analyzed, to have a further proof of the suitability of the algorithm for innovative concept missions. The thrusters selected for the chemical sizing are the bipropellant thruster ASTRIUM S400, as for the previous satellites, for primary propulsion, and ASTRIUM S10 for secondary propulsion, with specific impulse of 290 s, which use both hydrazine and Nitrogen Tetraoxide, and the monopropellant thruster ASTRIUM CHT400 and Moog

Table 4.2: Notional Mission 1 (NM1) Summary [3].

Objective	Design and execute Servicer missions to capture and relocate non-cooperative geosynchronous satellites.
Target Satellites	SDO, GOES, and others.
Capture Technique	Supervised AR&C with 2-meter robot arms.
AR&C Package	Mass: 141.1 kg, Power: 128.9 W, Data Rate: 996 Mbps (786 Mbps with compression).
Robot Arms	Four 2-meter arms for autonomous capture, Mass: 157kg each arm, Power: 380W each arm, teleoperated from ground (latency $<$ 3 seconds).
Spacecraft Design	3-axis stabilized, sun-pointing, fully redundant bus system with 1,500 W power, 100 Ahr Li-Ion batteries, and 250 Gbits data storage.
Propulsion	Chemical propulsion, dry mass: 2,352 kg, wet mass: 3,694 kg.
ΔV **budget**	Direct insertion in GEO, $11 m/s$ to reach the parking orbit, $48 m/s$ for nominal operations for each customer and $55 m/s$ per year for station keeping.
Mission Life	5 years
Number of Customers	10
Mission Control	NASA's Goddard Space Flight Center's SMOC

20N with 230 s of specific impulse for secondary propulsion, which use only hydrazine. The number of thrusters is 4 for the secondary propulsion and one for the primary. The main inputs are here summarized:

- **Payload mass**: 770 kg.
- **Payload power**: 1650 W. Where the peak operation was considered, in which all the 4 robotic arms operate contemporary at the maximum power.
- **Total ΔV budget**: 770 m/s, where also the station keeping is comprehended. Here the main hypothesis, is that the satellite is directly inserted in GEO with a dedicated launch with Atlas V.
- **Lifetime**: 5 years.
- **Prop system**:
  - **Bipropellant**:
    PRIMARY $T = 400N$, $I_{sp} = 318s$,
    SECONDARY $T = 10N$, $I_{sp} = 290s$,

PROPELLANTS $\rho_{MMH} = 880kg/m^3$, $\rho_{N_2O_4} = 1470kg/m^3$.

- **Monopropellant**:
  PRIMARY $T = 400N$, $I_{sp} = 220s$,
  SECONDARY $T = 22N$, $I_{sp} = 230s$,
  PROPELLANT $\rho_{MMH} = 880kg/m^3$.

4.1.4. Results comparison

Here, the results of the tool are compared with the ones obtained by the NASA study. The output is reported in the Table 4.3, but in order to properly compare the 2 results a change in the code has been made, by putting a 30% margin instead of the 20% defined in equation 2.45, which again shows the flexibility of the tool to be applied for a preliminary phase. It appears that the payload power alone is much higher than the total power obtained

	Dry mass(30% marg)	**Total mass**	**Total power**
NASA value	2350 kg	3700 kg	1500 W
Monopropellant	2576 kg	4318 kg	2860 W
Bipropellant	2361 kg	3550 kg	2860 W

Table 4.3: GEOdesign tool results for different thrusters

by the study. This discrepancy may be attributed to the interpretation of average power, as indicated in Table 4.2, or potential overestimation of the payload power. Without additional means of payload power estimation, it is suggested that the average power in the study may refer to the mean power used by the spacecraft between the lowest and highest consumption modes, resulting in a lower error than reported.

Table 4.3 reveals a high convergence achieved for the bipropellant case with the real dry mass of the satellite. Thus, it is likely that bipropellant propulsion is the selected option for the mission. However, an error of 150 kg is observed with the total mass, indicating a potential discrepancy in the input ΔV or in the thrusters selected. The resulting error is acceptable for the mission phase in which the tool is going to be used. However, to find a more accurate value, one should iterate by looking at different types of thrusters with slightly lower specific impulse than the ones selected or by adding specific margins to the maneuvers. After multiple attempts, it was found that the application of a 20% margin to the ΔV of the servicing maneuvers (client approach and Autonomous Rendez-vous and Capture (AR&C)), results in a more accurate sizing. The values with the addition of the margin are $M_{tot} = 3718kg$ and $M_{dry} = 2374kg$. This underscores the tool's utility for reverse engineering purposes in the context of innovative missions.

4.1.5. Propulsion trade-off

With the use of the tool it is also possible to perform a trade-off between the electrical and chemical propulsion, so in the next session a trade-off considering the new updated ΔV and the electric thrusters in 3.2 will be performed. In particular, the chance to perform also the GTO-GEO transfer. The enhancement of the number of possible customer serviced with respect to the chemical thrusters is instead difficult to be investigated, due to the lack of a AR&C study with low thrust for non-cooperative objects. Of course the maneuvers will not be instantaneous anymore and the orbit closing for the rendez-vous is more difficult with a low thrust solution, so a hybrid solution is presented, where the chemical propulsion is still present for the AR&C and disposal maneuvers. The criticality of the analysis consists in the absence of a dedicated low thrust mission analysis that could invalidate the ΔV values presented in the next section. However, here the fundamental hypothesis is that, given the low ΔVs considered in the single maneuvers of this phase, the differences between the retrieved values and the ones that could be computed with an optimization are negligible for the scope of the work.

GTO-GEO transfer upgrade

Even if the mass of the entire subsystem is already high, in order to lower the costs, one can better think to enhance the system by enabling the GTO to GEO transfer with the use of electric propulsion. The AR&C phase maneuvers and the disposal maneuver, once the spacecraft is docked, will be performed with the use of the secondary propulsion chemical thruster chosen for the previous phase, while the electric propulsion will be also used for the orbit change maneuvers between the different servicing periods and the station keeping. This choice, despite the mass penalty, will enable a GTO launch, that could result in an overall lowering of the sustained costs, due to the lowering of the launch costs, despite the insertion of electric thrusters, of additional solar panels and of additional propellant mass. As it is visible from the table 4.4, a GTO launch is more widely available, giving more freedom for the mission scheduling, but can also lower consistently the launch cost. The lowest cost can be around 11000€/kg if a ride-share configuration on a Falcon 9 or Falcon Heavy launch is chosen, against 48000€/kg if a GEO launch of a satellite, heavier than 5000 kg, is performed and the only available launcher compatible with the schedule is Delta IV Heavy.

The low thrust ΔVs for the maneuvers are evaluated, with an analytical formula derived with the use of several approximations. It is specific for continuous thrust maneuvers with a thrust vector perpendicular to the radial direction. The other hypothesis are: there is

	GTO P/L mass	GEO P/L mass	Launch cost
Ariane 62	4500 kg	None	70 M€
Ariane 64	11500 kg	5000 kg	115 M€
Falcon 9			
Reusable	5500 kg	None	62 M€
Expendable	8300 kg	None	Unknown
Falcon Heavy			
Reusable	8000 kg	3750 kg	89 M€
Expendable	26700 kg	6722 kg	138 M€
Delta IV Heavy	10100 - 14120 kg	6750 kg	320 M€

Table 4.4: Launchers characteristics. [4, 6, 11, 13, 55, 57, 61]

no inclination change between the maneuvers, the initial and final orbits are circular, the thrust is only in the transversal direction and, the strongest hypothesis, the thrust is constant during the transfer, which however is well suited to the brief maneuvers intended for this mission architecture. The derived formulas are the following [44]:

$$\Delta V = (1 - \frac{r_0}{r_f}) \cdot v_0 \tag{4.1}$$

Used if $r_0 < r_f$. And in the opposite case:

$$\Delta V = (\frac{r_0}{r_f} - 1) \cdot v_0 \tag{4.2}$$

Where r_0 and v_0 are the position and the velocity of the spacecraft in the first circular orbit and r_f is the radius of the final circular orbit. The resulting low thrust ΔV for the manuevers, from the parking orbit to the GEO and from the disposal orbit back to the parking one for 10 clients is of 300 m/s. The remaining chemical ΔV for the AR&C and the disposal of 10 clients is of 350 m/s. To the electrical ΔV must be added also the station keeping already presented and the GTO-GEO transfer, with the margin of 1.4[22] already presented. This can change between 1500 m/s if the GTO inclination is around 6° degrees (Ariane 6, Delta IV Heavy highest payload mass) and 1800 m/s if the inclination is around 28°, prior to the margin application. The number of thruster selected is 3 for SPT 100 D and 2 for XIPS 25 and PPS 5000, whose characteristics are enlisted in the Table 3.4. **It is evident from Table ?? that opting for a hybrid solution with orbit raising conducted by electric thrusters consistently results in lower launch costs for this specific mission. The potential savings can reach around 40 million euros, especially when launching from Geosynchronous Transfer Orbit (GTO) using Falcon 9 compared to Ariane 64 in Geostationary orbit**

(GEO). This calculation takes into account the cost difference in satellite production as well. The value $\Delta cost_{sat}$ is a cost difference between the chemical satellite launched in GEO and the hybrid satellite launched in GTO. The exact coefficients used for the evaluation of these costs cannot be shown, because are property of D-Orbit. The evaluation of the costs was based on three main function, structured as follows.

$$\Delta EPS_{cost} = f(\Delta P_{tot}) \tag{4.3}$$

$$\Delta PS_{cost} = f(\Delta M_{ox}, \Delta M_{fu}, M_{Xe}, N_{ELthrusters}, \Delta N_{CHEMthrusters}) \tag{4.4}$$

Where, $M_{Xe}, N_{ELthrusters}, N_{CHEMthrusters}$ are, respectively, the Xenon mass, the number of electric thrusters and the number of chemical thrusters, differenced by thrust. So, it was not taken into account the growth of the cost based on the variation of the other subsystems' variations, but one can state that, as the main point of the entire thesis has demonstrated, the most important differences in terms of masses and powers are linked to EPS and PS subsystems.
This type of thruster requires a higher time for the orbit raising, with respect to the others, but always below a transfer duration of one year. This was the driver in the selection of the number of thrusters (simply estimated by dividing the ΔV by the acceleration at Beginning of Life and considering a 90% of duty cycle[20]). The biggest drawback in this solution is the increase of the panels area, resulting from the power increase that can lead to $43m^2$ for the XIPS 25 and PPS5000 solutions. This increase can be a too strict limitation for the proximity operations. As a consequence, one can think to install a retraction mechanism for the proximity operations (with the drawback to be less reliable) or simply to mount less thrusters or less powerful thrusters by increasing the transfer time and the shielding needed. However, these deeper analyses on the technical criticalities of the proposed solutions are outside the scope of this work and are to be done by the system engineer outside the tool. This trade off can be exploited much faster than the usual methods and by also trading off at the same time with the mission operations. In this case, for example, it is clear that no ride-sharing is permitted, because it is unlikely to find a 1500 kg satellites that reaches GTO. So, one can trade off to service more satellites, by adding the corresponding ΔV needed for each excess satellite and by adding the corresponding lifetime increase in input to the tool, and see how many more clients can be served and full the payload fairing. This is a further proof of the role of this tool as the enabler for the financial sustainability of the next generation IOS satellites. The results for PPS5000 are not reported under the section of Ariane 62 in the Table 4.5, because the output total mass is higher than the launcher maximum payload mass. For

	M_{dry}	M_{tot}	P_{tot}	Launch cost	$\Delta cost_{sat}$
Ariane 64					
GEO chemical value	2350 kg	3700 kg	1500 W	115 M€	0 €
Ariane 62					
XIPS 25	3264 kg	4404 kg	11 kW	70 M€	+5.3 M€
SPT 100 D	2952 kg	4155 kg	7.5 kW	70 M€	+6.2 M€
Falcon Heavy					
GEO chemical value	2350 kg	3700 kg	1500 W	89 M€	0 €
Falcon 9					
XIPS 25	3280 kg	4485 kg	11 kW	62 M€	+5.7 M€
PPS 5000	3402 kg	4955 kg	11.5 kW	62 M€	+6.8 M€
SPT 100 D	2977 kg	4278 kg	7.5 kW	62 M€	+7.8 M€

Table 4.5: GEOdesign tool results comparison for GEO chemical and GTO hybrid solutions.

a further comparison, the same tradeoff has been performed with all chemical satellites launched in GTO, but the resulting spacecraft were too heavy to be launched with Ariane 62 and Falcon 9, resulting in a lower competitive advantage with respect to the ones already shown.

4.2. Mission scenario 2

As a reference for the second mission scenario, the Notional Mission 2 (NM2) developed by NASA[3], was taken into account. It focuses on developing a mission concept for in-orbit refueling of multiple Customer spacecraft at GEO. The mission involves two satellites: the Refueler and the Fuel Depot. The Refueler, a small and agile spacecraft, refuels five Customer satellites during each sortie and rendezvous with the Fuel Depot for refueling between sorties. The Fuel Depot, a minimalist design, carries enough fuel for the Refueler to service up to 25 Customer satellites. The mission assumes launch in 2015, with a 10-year mission life.

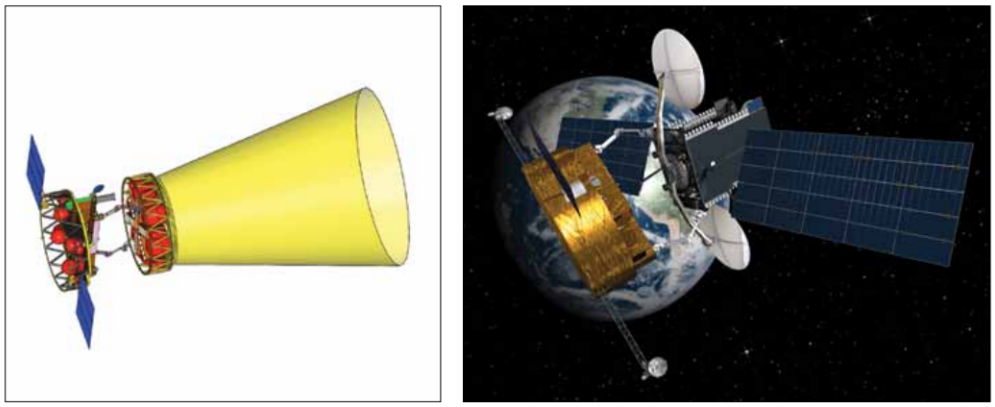

Figure 4.3: Refueler docked to the depot (left), Refueler docked to a customer (right) (Credit: NASA).

4.2.1. Mission Details

Table 4.6: Notional Mission 2 (NM2) Components

Refueler	Small and agile spacecraft designed to refuel five Customer satellites during each sortie
Fuel Depot	Passive spacecraft with minimal subsystems, carries fuel for up to 25 Customer satellite refuelings
Launch Configuration	Launched together on a Delta IV Heavy to 100 km above GEO
Mission Life	10 years

Key Assumptions

- Customer satellites have attitude rates less than 0.25 deg/sec/axis.
- Refueler solar array has at least 30% illumination.
- Two toolboxes on the Refueler are adequate to refuel five Customer satellites at a time.
- Six additional toolboxes on the Depot are sufficient for refueling follow-on Customer satellites.

4.2.2. System Description

The mission comprises the Refueler and the Fuel Depot. The Refueler, weighing 1,894 kg (including 30% contingency), carries a modified AR&C system (without a pan/tilt

unit but with four extra cameras), two robot arms, two toolboxes, and the refueling system/package. After initial separation from the Depot, the Refueler raises its orbit from GEO + 100 km to GEO + 127 km, drifting between Customer spacecraft. When within 300 km of a Customer, it lowers its orbit to GEO – 30 km to initiate the AR&C sequence, expending 20 m/s of ΔV. After capturing and refueling the Customer, the Refueler drifts to the next Customer. This cycle repeats until six Customers receive 20 kg of propellant each. After refueling, the Refueler performs AR&C with the Depot, corrects its orbit plane, tops off its fuel, and continues sorties. The Refueler and Depot stack boosts to GEO + 300 km for disposal.

Table 4.7: Refueler Specifications [3]

Dry Mass	1,894 kg (includes 30% contingency)
Components	Modified AR&C system, two robot arms, two toolboxes, refueling system/package
Refueling system characteristics	Maximum propellant payload of 120 kg (20 kg for 6 clients) and 7 kg of Titanium spherical tank
Robotic system characteristic	From table 4.2. AR&C system mass: 141.1 kg, AR&C system power: 128.9 W. Two 2-meter arms for autonomous capture, Mass: 157kg each arm, Power: 380W each arm, teleoperated from ground (latency $<$ 3 seconds).
ΔV **budget**	20 m/s for each AR&C sequence, 5.6m/s for each client approach, 2.1 m/s for each depot approach 6.3 m/s for disposal. For a total of 945 m/s for operations for 25 satellites and for 5 trips to the refueler spacecraft. A further budget for 54 m/s of station keeping per year is assumed, with the refueler that performs the station keeping on the depot, once docked. The results are obtained with the sizing of Hohmann transfers between the orbits shown in figure 4.4, except for the rendezvous and capture, which is given [3].
Power Source	7.2 m^2 solar array, 2 x 100 Ah Li-Ion JSB batteries
Communication	S-band Omni, X-band HGA (10 Mbps downlink)

In this mission, the Refueler autonomously captures and refuels Customer satellites using its robot arms and toolboxes, demonstrating a comprehensive solution for in-orbit refueling in GEO. It is assumed that the same robotic arm of the previous mission scenario is utilized. However, the case study will be only done for the Refueler, because as can be seen from Table 4.8, the components of the depot are too different from the communication satellites architecture utilized in the statistics. The ADCS of the depot is passive,

Table 4.8: Fuel Depot Specifications[3]

Dry Mass	1,326 kg (includes 30% contingency)
Components	Composite truss design, MLI, heaters, thermistors, no RF communication, passive ADCS with solar sail. Hidrazine propellant and N2 pressurant as payload.
Toolboxes	Six toolboxes for servicing Customer satellites

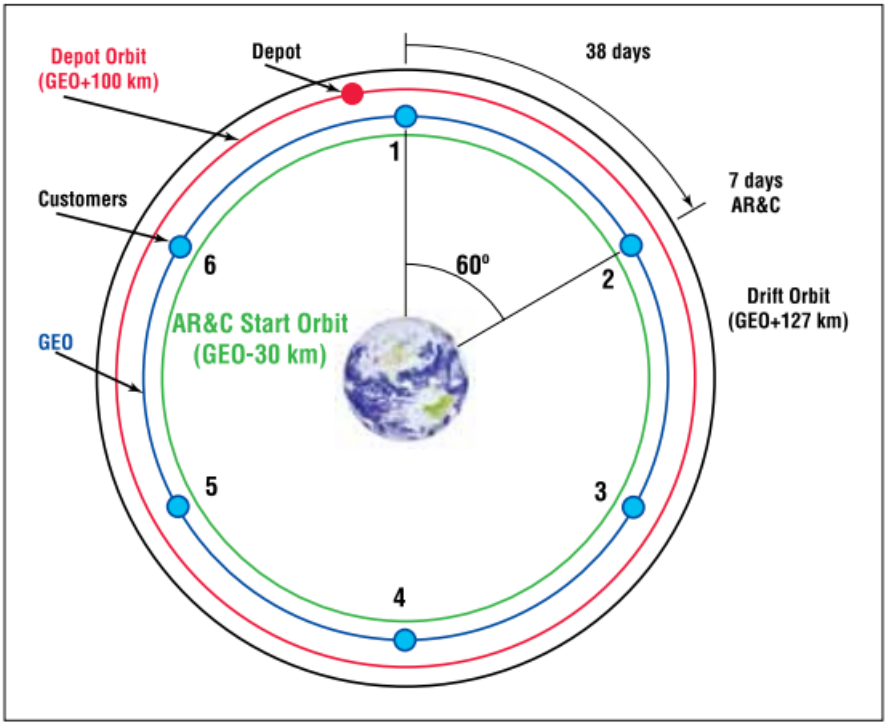

Figure 4.4: Refueling mission scenario (Credit: NASA)

differently from the tool. There is no RF communication and no heat pipes are there in the depot. There are also no avionics and batteries, leading to a unique design of the depot satellites. It is basically a tank, with interfaces for the docking and with solar panels, that give energy to the thermal control devices. This leads to the invalidation of the hypothesis of the tool expressed in section 2.1. Another problem would be that the mass of the six toolboxes services for the Refueler is unknown, and the range of payload mass, due to the high quantity of fuel can be out of the limitations imposed.

4.2.3. Input

As before, the main inputs are extrapolated from the Tables 4.2 and 4.7, and the same set of thrusters of the previous section is utilized. The input for the Refueler sizing can be summarized as follows:

- **Payload mass**: 582 kg, which takes into account, the robotic arms, the $AR\&C$ system, and the 120 kg of fuel that will be delivered to the 6 clients satellites, between two consecutive refuelings at the depot, and 7 kg of Titanium tank to contain the fuel.
- **Payload power**: 890 W. Where the peak operation was considered, in which the 2 robotic arms operate contemporary at the maximum power, together with AR&C sensor system.
- **Total ΔV budget**: 245 m/s for transfer and 108 m/s for station keeping, where is considered that the station keeping is performed at the docking with the depot at the end of the operations. The ΔV is different from the table 4.7, because it is considered that the satellite goes to the depot to refuel itself, once every 5 customers, so only the maneuevers needed for the refueling of 5 customers and the back and forth to the depot station are considered.
- **Lifetime**: 10 years.
- **Prop system**:
  - **Bipropellant**:
    PRIMARY $T = 400N$, $I_{sp} = 318s$,
    SECONDARY $T = 10N$, $I_{sp} = 290s$,
    PROPELLANTS $\rho_{MMH} = 880kg/m^3$, $\rho_{N_2O_4} = 1470kg/m^3$.
  - **Monopropellant**:
    PRIMARY $T = 400N$, $I_{sp} = 220s$,
    SECONDARY $T = 22N$, $I_{sp} = 230s$,
    PROPELLANT $\rho_{MMH} = 880kg/m^3$.

The bipropellant is shown in the comparison just to look at the differences between the 2 systems, because it is a priori known that the spacecraft system is a monopropellant. This is due to the operations needed, when the spacecraft docks to the depot, the fuel taken is for both the maneuvers that will be executed in the following 2 years and fot the customer satellites. In addition, the N2 pressurizer is loaded together with the propellant for the spacecraft operations. So, knowing that the depot carries only Hydrazine and

Nitrogen, it is obvious that a monopropellant system is used.

4.2.4. Results comparison

Differently from the NM1 case, here no information is given on the total power of the satellite, but the total area of the solar panels is known, so the comparison will be conducted on that value. As before, a margin of 30% is applied to the dry mass for a fair comparison with the paper values. The results in Table 4.9 demonstrate the effectiveness

	Dry mass(30% marg)	**Propellant mass**	**SA power**	**SA area**
NASA value	1894 kg	unknown	unknown	7.2 m^2
Monopropellant	1898 kg	543 kg	1890 W	8.8 m^2
Bipropellant	1837 kg	401 kg	1890 W	8.8 m^2

Table 4.9: GEOdesgin tool results for different thrusters, for refueling mission

of the tool in providing precise estimates for the dry mass of the satellite. Furthermore, the tool allows for trade-offs between different operational concepts, as seen in the case of choosing between monopropellant and bipropellant systems. The tool suggests a potential overall mass saving of 570 kg by opting for a bipropellant system, but it also highlights the increased complexity and operational risks associated with this choice.

Despite a slight mismatch in the solar panels area, it is acknowledged that this discrepancy could be attributed to uncertainties in the payload power. Specifically, the paper [3] currently provides the peak power of a single arm, while the total power during the operations of both arms is not known. This contributes to the overall uncertainty in the results.

In summary, the tool offers a means to obtain mass and power budgets for IOS spacecraft with acceptable precision, given the knowledge of operations and payload. It facilitates rapid and precise trade-offs between different operational concepts compared to standard methods. By using the tool, the focus can be directed toward operations and payload definition, streamlining the preliminary design process.

The tool also proves useful in extracting information from missions, even when specific details are not available. For example, the tool retrieved the propellant mass of the spacecraft for each sortie after evaluating the ΔV with simple Hohmann transfers. This led to a total propellant mass of 2715 kg, enabling the sizing of the depot spacecraft. However, it is reiterated that the depot cannot be fully sized using this tool due to its unique characteristics, and the payload mass remains out of range for the tool. For this case a GTO - GEO transfer enhancement, with the use of electric propulsion is less suited

than before, due to the peculiar servicing characteristics, which suggests the only use of monopropellant thrusters. However, the total mass of the depot and the servicer together is around 6480 kg, by adding the total propellant mass evaluated per each sortie and the depot dry mass, from [3]. As a consequence, the launch can only be made with Delta IV Heavy or Atlas V or Falcon Heavy. In line with what has been suggested in the previous case study, in order to avoid to launch with Delta IV Heavy (which has a cost of 350 M€, as reported in 4.4), one can trade off with the number of customers serviced. By serving less clients, one can save as much as 200 M€, just for the launch. With the use of the tool for this trade off, one can quickly retrieve the number of clients to be served to be launched with Ariane 64, and trade-off by knowing the servicing income. If one can launch with Falcon Heavy, then the cost is around 138 M€, for the expendable launch configuration, leading to the least consumption for this type of architecture, without any changes. The mass is in line with Falcon Heavy payload limitation, because it has been retrieved from previous launches, that Falcon Heavy is capable of transporting a payload of at least 6722 kg[13] in GEO.

In conclusion, the tool offers significant time savings in the preliminary design of space architectures. It allows designers to focus on operational concepts and explore different options efficiently.

5 | Conclusions and future developments

The present work has demonstrated the feasibility in the creation of a fast preliminary sizing tool for architectures in geostationary orbit. Despite the use of statistical relations of datasets composed only by communication satellites, the tool has been demonstrated to be effective and to be superior to the already existing preliminary sizing statistical relations in the budgeting of non-communication satellites, with acceptable performances. Due to the limitations imposed in the payload type and in the payload mass, it has been demonstrated the possibility to design preliminary architectures for GEO IOS missions, which was the main scope of the work. Hereafter the tool's benefits, limits and possible future developments will be exposed.

Benefits of the tool

- The GEOdesign tool has proven to be faster than traditional methods for preliminary design.
- It offers an acceptable level of accuracy, with respect to the early phase of the design in which it can be used, even superior to statistical relations found in the literature and comparable to mission designs conducted by NASA researchers.
- It is of great help for the maneuvering strategy definition performed by the mission analyst by giving the change also in the dry mass of the spacecraft, once the payload of the mission is defined.
- With the use of this tool, the attention can be shifted towards the operations of the mission, by instantaneously analyzing the effects on the entire architecture caused by the insertion of a different maneuvering strategy or of a different servicing time or by the increase of serviced satellites.
- High level trade offs, regarding the choice of the insertion orbit and of the type of propulsion, can be performed faster than before, resulting in a conspicuous cost-

effective advantage, has as been shown in the case study chapter.

- The GEOdesign tool does not require the entire designing team to be reunited and to reiterate the work, to perform the trade-offs already cited.

Limits of the tool

- The input payload mass is constrained between 130 and 650 kg for chemical and hybrid satellites and between 140 and 1500 kg for all-electric satellites, due to the input limitations in the databases used. In addition, a limitation in the satellite output mass, is associated to the input one, without the possibility to design small-sized spacecrafts.
- Restrictions on the types of spacecraft that can be sized. For instance, it cannot accommodate peculiar spacecraft types like the depot spacecraft presented in the second mission scenario, which lacks a TTMTC system, propulsion system, and has a passive ADCS. The first limitation is intrinsically linked to a restricted selection of the type of payload that can be used. A single tether for the debris removal is for example not feasible to be used in the design, due to the low mass associated. As a result, the tool is well suited for the sizing of IOS spacecraft with robotic arms of certain dimensions, and for the sizing of refueler spacecrafts with a limited amount of fuel, that probably rely on a Depot satellite or on a mother station to pick up the fuel.
- The subsystems' budgets have not been validated due to lack of exact information in literature.
- The technical limitations of the solutions proposed, like for example the maneuvering constraints imposed by larger solar arrays, must be determined by the engineering team outside the tool.

Future Developments

In terms of future developments, the tool can be enhanced in the industrial perimeter under the following aspects:

- It could be expanded to cover a broader range of orbits and accommodate various spacecraft types.
- A more in-depth statistical analysis of subsystems not currently modeled could be undertaken.

- Integration with a mission analysis tool to form an optimizer for in-orbit servicing missions is another avenue for improvement. This would provide the entire mission profile as output, including the number of satellites that can be serviced based on propellant payload, and enable trade-offs on thruster selection.
- The addition of a cost model that can enable a cost trade off as a direct output of the tool, that brings to an exact evaluation of the minimum price to apply to the single servicing. Consequently, the tool can be inserted into an optimizer to evaluate the optimal mission architecture to obtain a certain revenue.
- The development of a graphic user interface, to make the tool user-friendly.

Under the academical point of view, further enhancements may involve expanding payload limitations by incorporating specific sets of relations for more and less massive payloads. The tool could offer a choice between different payload characteristics, leading to entirely different relations and sizings. For example, when sizing a depot, knowing the propellant mass would simplify the process to structural and thermal considerations only, with a set of equations distinct from those presented in this work. This would lead to the possibility of designing more innovative mission concepts and scenarios, which can be too advanced for the current technology readiness level, which is instead a priority in the risk mitigation on the industrial side. A further option is to add specific relations with the use of SPace ENVironment Information System (SPENVIS), that relate a mass increase for the shielding proportional to the time spent for the GTO - GEO transfer, which is partially taken into account for the electric satellites but not for the hybrid ones.

In conclusion, the use of this tool provides a significant advantage for companies exploring concepts for in-orbit servicing satellites. It grants system engineers the flexibility to evaluate mission operations freely, delivering precise and rapid responses on system architectures once the payload is selected.

Bibliography

[1] A. F. Abad, O. Ma, K. Pham, and S. Ulrich. A review of space robotics technologies for on-orbit servicing, 2013.

[2] P. Abbasrezaee, M. Mirshams, and S. Zamani. Conceptual geo telecommunication all-electric satellite design based on statistical model, 2019.

[3] N. Aeronautics and S. A. G. S. F. Center. On-orbit satellite servicing study, 2010.

[4] AEROSPACE. Ussf-44: Space force successfully completes first mission on falcon heavy rocket, 2022. URL `https://aerospace.org/article/ussf-44-space-force-successfully-completes-first-mission-falcon-heavy-rocket`.

[5] ArianeSpace. Ariane 5 user's manual issue 5 revision 2, 2016.

[6] ArianeSpace. Ariane 6 user's manual issue 2 revision 0, 2021.

[7] G. Baldesi, A. Califano, M. D. Marco, G. G. E. Di Litta, S. Mezzasoma, and G. Orlando. Mastersat b: Mission and analysis design. Master's thesis, Università degli Studi di Roma "La Sapienza", 2003.

[8] E. Bourguignon and S. Fraselle. Power processing unit activities at thales alenia space in belgium. *International Electric Propulsion Conference*, 2019.

[9] J. R. Brophy. Stationary plasma thruster evaluation in russia. Technical report, NASA JPL, 1992.

[10] Brown. *Elements of Spacecraft Design*. AIAA, 2002.

[11] T. Bruno. Greetings to elon musk, 2018. URL `https://twitter.com/torybruno/status/963109303291854848`.

[12] Y.-K. Chang, K.-L. Hwang, and S.-J. Kang. Sedt (system engineering design tool) development and its application to small satellite conceptual design, 2007.

[13] J. Davenport. Viasat-3 americas launches on expendable falcon heavy, 2023. URL `https://www.nasaspaceflight.com/2023/04/viasat-3-americas/`.

[14] M. Drube, H. Gray, and A. Demaire. Plasma propulsion system functional chain validation on eurostar 3000. *Research Gate*, 2003.

[15] ECSS. Ecss-e-st-10c rev.1 - system engineering general requirements - secretariat esa-estec requirements & standards division. Technical report, ECSS, 2017.

[16] eoPortal. Satellite missions catalogue, 2023. URL `https://www.eoportal.org/satellite-missions`.

[17] ESA. Margin philosophy for science assessment studies. Technical report, ESA - SRE-PA & D-TEC staff, 2012.

[18] ESA. Present and future of space electric propulsion in europe, 2018.

[19] M. Fakoor, S. M. N. Ghoreishi, and H. Sabaghzadeh. Spacecraft component adaptive layout environment (scale): An efficient optimization tool, 2016.

[20] C. Feola. Analisi delle condizioni di ottimo per traiettorie spaziali con discontinuità di spinta, 2022.

[21] M. Fick et al. Eads-st's latest bipropellant 10n thruster and 400n engine: the fully european solution. *4th International Spacecraft Propiulsion Conference*, 2004.

[22] M. J. Glogowski, J. D. Anderson, G. A. Herbert, A. D. Kodys, and W. A. Llorens. Application of solar electric propulsion in the emerging satellite servicing industry. *Presented at the 36th International Electric Propulsion Conference, Vienna*, 2019.

[23] D. M. Goebel, J. E. Polk, I. Sandler, I. G. Mikellides, J. Brophy, W. G. Tighe, and K.-R. Chien. Evaluation of 25-cm xips thruster life for deep space mission applications. *IEPC*, 2009.

[24] G.Ridolfi, E.Mooij, and S.Corpino. A system engineering tool for the design of satellite subsystems, 2009.

[25] Gunterspace. Chronology of space launches, 2023. URL `https://space.skyrocket.de/directories/chronology.htm`.

[26] J. T. Hwang, D. Y. Lee, J. W. Cutler, and J. R. R. A. Martins. Large-scale multidisciplinary optimization of a small satellite's design and operation, 2014.

[27] R. Lombardi. *Design, Simulation, Management and Control of a Cooperative, Distributed, Earth-Observation Satellite System*. PhD thesis, Politecnico di Milano, 2014.

[28] M. Macdonald and V. Badescu. *The International Handbook of Space Technology*. Springer, 2014.

[29] D. Malyh, S. Vaulin, V. Fedorov, R. Peshkov1, and M. Shalashov. A brief review on in-orbit refueling projects and critical techniques, 2021.

[30] D. Manzella. Performance evaluation of the spt-140. Technical report, NASA JPL, 1997.

[31] Y. MATSUNAGA, T. TAKAHASHI, H. WATANABE, D. GOTO, S. CHO, H. KUSAWAKE, F. KUROKAWA, K. KAJIWARA, and I. FUNAKI. Wide-output range power processing unit for 6-kw hall thruster. *IEEE TRANSACTIONS ON AEROSPACE AND ELECTRONIC SYSTEMS*, 2022.

[32] A. I. McInnes, D. M. Harps, J. A., and Lang.v. A system engineering tool for small satellite design, 2001.

[33] D. V. McKinnon, H. Weigl, and L. Maack. Lockheed martin's a2100 spacecraft bus modernization. Technical report, Lockheed Martin Space Systems Company, 2015.

[34] M. Mirshams and E. Zabihian. Fadsat: A system engineering tool for the conceptual design of geostationary earth orbit satellites platform. *Journal of Aerospace Engineering*, 233(6) 2152–2169, 2019.

[35] M.Oda, K.Kibe, and F.Yamagata. Ets-vii, space robot in-orbit experiment satellite, 1996.

[36] NIST. Thermophysical properties of fluid systems, 2023. URL `https://webbook.nist.gov/chemistry/fluid/`.

[37] NOOA. Goes eclipse schedule -n.o.o.a. office of satellites and product operations, 2023. URL `https://www.ospo.noaa.gov/Operations/GOES/eclipse.html`.

[38] OHB. Satellite platforms: Medium and large platforms, 2018.

[39] Orbital-ATK. Geostar-3 bus, 2016.

[40] H. Osuga, K. Suzuk, T. Ozaki, T. Nakagawa, I. Suga, T. Kawakam, T. Sakai, Y. Akuzawa, F. Soga, and T. Furuich. Development status of power processing unit for 200mn-class hall thruster. *International Electric Propulsion Conference*, 2005.

[41] P.Abbasrezaee and A. Saraaeb. System analysis and design of the geostationary earth orbit all-electric communication satellites. *Journal of Aerospace Technology and Management*, 2021.

[42] C. A. Paissoni. *Comprehensive Approach to Electric Propulsion for Innovative Space Platforms*. PhD thesis, Politecnico di Torino, 2021.

[43] J.-F. Poussin and G. Berger. Eurostar e3000 three-year flight experience and perspective. *AIAA (American Institute of Aeronautics and Astronautic)*, 2007.

[44] J. Prinetto. Low thrust trajectories design and optimization - sseo course, 2021.

[45] Y. Qiu, B. Guo, L. Xue, B. Liang, and C. Li. On-orbit servicing to geo satellite using dual arm free-flying space robot, 2009.

[46] S. Rajkumar, D. Ravindran, K. A. Raj, and K. P. Shetty. Experimental investigation of stiffness characteristics of tee joints of aluminum honeycomb core sandwich panels with different edging configurations. *International Conference on Applications and Design in Mechanical Engineering*, 2012.

[47] Reader. Ae1222-ii: Aerospace design systems engineering elements i - part: Spacecraft (bus) design and sizing, 2014.

[48] G. Ridolfi, E. Mooij, and S. Chiesa. A parametric approach to the concurrent design of complex systems, 2010.

[49] Saab. Saab - spacecraft management unit, 2005.

[50] SAFRAN. Pps 5000 stationary plasma thruster - safran spacecraft propulsion, 2019.

[51] SAFRAN. Pps x00 stationary plasma thruster - safran spacecraft propulsion, 2019.

[52] J. M. Sankovic, J. A. Hamley, and T. W. Haag. Performance evaluation of the russian spt-100 thruster at nasa lerc. Technical report, NASA, 1993.

[53] SETS. Ppu 500, unknown year.

[54] SETS. St-100 hall-effect thruster, unknown year.

[55] M. Sheetz. Tech - elon musk says the new spacex falcon heavy rocket crushes its competition on cost, 2018. URL `https://www.cnbc.com/2018/02/12/elon-musk-spacex-falcon-heavy-costs-150-million-at-most.html`.

[56] R. Shi, L. Liu, T. Long, J. Liu, and B. Yuan. Large-scale multidisciplinary optimization of a small satellite's design and operation, 2017.

[57] R. Smith. Europe complains: Spacex rocket prices are too cheap to beat, 2018. URL `https://www.fool.com/investing/2018/06/02/europe-complains-spacex-rocket-prices-are-too-chea.aspx`.

[58] T. A. Space. Gotofly! catalogue of iod/iov carriers, 2015.

[59] Space-Systems-Loral. Ssl 1300 spacecraft bus for rsdo applications, unknown.

[60] Spaceflight101. Satellite library, 2023. URL https://spaceflight101.com/spacecraft/.

[61] SpaceX. Falcon user's guide, 2021.

[62] TopTech. Mediaglobe study in tu delft, 1999.

[63] UCS. Ucs satellite database - union of concerned scientists, 2023. URL https://www.ucsusa.org/resources/satellite-database.

[64] Wertz. Space mission analysis and design, 2013.

[65] W. Xu, B. Liang, B. Li, and Y. Xu. A universal on-orbit servicing system used in the geostationary orbit, 2011.

[66] P. M. Zadeh and M. S. Shirazi. Multidisciplinary design optimization architecture to concurrent design of satellite systems, 2016.

[67] Y. Zhao, X. Chen., and Z. Wang. Sidea tool for integrated multidisciplinary design optimization of spacecraf, 2006.

List of Figures

List of Tables

Acknowledgements

I would like to express my gratitude to D-Orbit for providing me with this valuable opportunity and for their continuous technical support and provision of data throughout the entire duration of the internship. A special acknowledgment goes to my supervisor, Salvatore Andrea Bella, for his unwavering commitment and dedicated guidance. Without his support, this work would have been impossible to accomplish.